Low export flux of particulate organic carbon in the central Arctic Ocean as revealed by ^{234}Th:^{238}U disequilibrium

P. Cai,[1] M. Rutgers van der Loeff,[2] I. Stimac,[2] E.-M. Nöthig,[2] K. Lepore,[3] and S. B. Moran[4]

Received 24 June 2009; revised 11 May 2010; accepted 27 May 2010; published 16 October 2010.

[1] The loss of Arctic sea ice has accelerated in recent years. With the decline in sea ice cover, the Arctic Ocean biogeochemistry is undergoing unprecedented change. A key question about the changing Arctic Ocean biogeochemistry is concerning the impact of the shrinking sea ice cover on the particulate organic carbon (POC) export from the upper Arctic Ocean. Thus far, there are still very few direct measurements of POC export in the permanently ice-covered central Arctic Ocean. A further issue is that the magnitude of the POC export so far documented in this region remains controversial. During the ARK-XXII/2 expedition to the Arctic Ocean from 28 July to 7 October in 2007, we conducted a high-resolution study of POC export using ^{234}Th/^{238}U disequilibrium. Depth profiles of total ^{234}Th in the upper 200 m were collected at 36 stations in the central Arctic Ocean and its adjacent seas, i.e., the Barents Sea, the Kara Sea and the Laptev Sea. Samples were processed using a small-volume MnO_2 coprecipitation method with addition of a yield tracer, which resulted in one of the most precise ^{234}Th data sets ever collected. Thorium-234 deficit with respect to ^{238}U was found to be evident throughout the upper 100 m over the Arctic shelves. In comparison, ^{234}Th deficit was confined to the upper 25 m in the central Arctic Ocean. Below 25 m, secular equilibrium was approached between ^{234}Th and ^{238}U. The observed ^{234}Th deficit was generally associated with enhanced total chlorophyll concentrations, indicating that in situ production and export of biogenic particles are the main mechanism for ^{234}Th removal in the Arctic Ocean. Thorium-234-derived POC fluxes were determined with a steady state model and pump-normalized POC/^{234}Th ratios on total suspended particles collected at 100 m. Results showed enhanced POC export over the Arctic shelves. On average, POC export fluxes over the various Arctic shelves were 2.7 ± 1.7 mmol m^{-2} d^{-1} (the Barents Sea), 0.5 ± 0.8 mmol m^{-2} d^{-1} (the Kara Sea), and 2.9 ± 1.8 mmol m^{-2} d^{-1} (the Laptev Sea) respectively. In comparison, the central Arctic Ocean was characterized by the lowest POC export flux ever reported, 0.2 ± 1.0 mmol m^{-2} d^{-1} (1 standard deviation, n = 26). This value is very low compared to prior estimates and is also much lower than the POC export fluxes reported in other oligotrophic oceans. A ThE ratio (^{234}Th-derived POC export/primary production) of <6% in the central Arctic Ocean was estimated using the historical measurements of primary production. The low ThE ratio indicates that like other oligotrophic regimes, the central Arctic Ocean is characterized by low POC export relative to primary production, i.e., a tightly coupled food web. Our study strongly suggests that the current role of the central Arctic Ocean in C sequestration is still very limited. Meanwhile, this role might be altered because of global warming and future decline in sea ice cover.

Citation: Cai, P., M. Rutgers van der Loeff, I. Stimac, E.-M. Nöthig, K. Lepore, and S. B. Moran (2010), Low export flux of particulate organic carbon in the central Arctic Ocean as revealed by ^{234}Th:^{238}U disequilibrium, *J. Geophys. Res.*, *115*, C10037, doi:10.1029/2009JC005595.

[1]State Key Laboratory of Marine Environmental Science, Xiamen University, Xiamen, China.
[2]Alfred-Wegener Institute for Polar and Marine Research, Bremerhaven, Germany.
[3]School of Physics, University College Dublin, Dublin, Ireland.
[4]Graduate School of Oceanography, University of Rhode Island, Narragansett, Rhode Island, USA.

0148-0227/10/2009JC005595

1. Introduction

[2] The loss of Arctic sea ice has accelerated in recent years. Satellite data revealed that the extent and area trends of the entire Arctic sea ice cover have shifted from about −2.2% and −3.0% per decade in 1979–1996 to about −10.1% and −10.7% per decade in the last 10 years [*Comiso et al.*, 2008]. Recent results from modeling studies suggested that

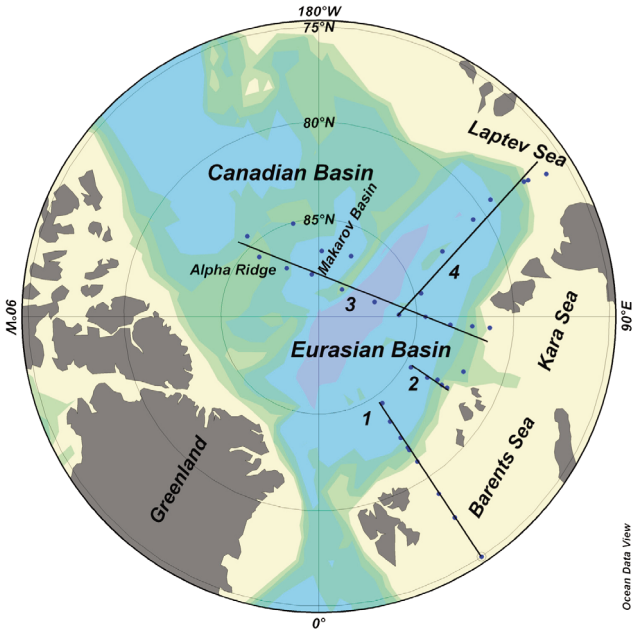

Figure 1. Map of the Arctic Ocean. Sampling stations from the ARK-XXII/2 expedition in 2007 are indicated by solid circles. The coordinates of the sampling stations can be found in Table 1.

there is a high probability of a 40% reduction of summer sea ice extent (relative to the 1979–1999 mean) in the Arctic by the year 2050 [*Overland and Wang*, 2007]. With the decline in sea ice cover, the Arctic Ocean biogeochemistry is undergoing unprecedented change. The Arctic Ocean CO_2 sink was estimated to have tripled between 1972 and 2002, from 24 Tg yr^{-1} to 66 Tg yr^{-1}. By the year 2012, this sink was supposed to increase by an additional 20 ± 3 Tg yr^{-1} [*Bates et al.*, 2006]. Annual primary production, in the meantime, has increased by an average of 27.5 Tg yr^{-1} since 2003 and by 35 Tg yr^{-1} between 2006 and 2007, when the lowest sea ice cover and the largest single year drop in minimum sea ice extent by far were recorded [*Arrigo et al.*, 2008].

[3] A key question is to what extent will the shrinking sea ice cover impact the particulate organic carbon (POC) export from the upper Arctic Ocean? While there have been a number of studies on POC export in the Arctic seas [*Moran and Smith*, 2000; *Wassmann et al.*, 2004; *Moran et al.*, 2005; *Lepore et al.*, 2007; *Lalande et al.*, 2007, 2008], direct measurements of POC export in the permanently ice-covered central Arctic Ocean are still very sparse, primarily because of logistic difficulties. A further issue is that the magnitude in POC export estimates so far documented in this region remains controversial. On the basis of the sediment trap record, *Hargrave et al.* [1994] demonstrated that under the permanent ice cover, mean annual POC export flux from the upper 100 m can be as low as 0.03 ± 0.02 mmol m^{-2} d^{-1}. In contrast, other studies using $^{234}Th/^{238}U$ disequilibrium generally suggested a much higher POC export in the central Arctic Ocean [e.g., *Moran et al.*, 1997; *Baskaran et al.*, 2003]. Thus, it is of critical importance to derive high-resolution high-precision estimates of POC export before the Arctic summer sea ice has completely disappeared.

[4] In this study, we utilized the disequilibrium between ^{234}Th and its parent nuclide, ^{238}U, to estimate the POC export from the upper Arctic Ocean. The short-lived ^{234}Th has a half-life ($t_{1/2}$) of 24.1 days and is very particle reactive. In the open ocean, it is produced from ^{238}U at a nearly constant rate. The basis of the ^{234}Th method for quantifying the upper ocean POC export is relatively straightforward: the deficit of ^{234}Th with respect to ^{238}U in seawater is mainly due to removal by scavenging onto sinking particles. Thorium-234 fluxes are converted into POC export rates by simply multiplying the ^{234}Th flux by the POC/^{234}Th ratio on sinking particles at the depth horizon of interest [*Buesseler et al.*, 2006]. In particular, recent development of the small-volume technique has enabled the ^{234}Th method to provide a detailed view into POC export in the upper ocean that is difficult to obtain with other approaches [e.g., *Buesseler et al.*, 2005; *Cai et al.*, 2008a].

2. Methods

2.1. Sample Collection

[5] Water samples were collected during the ARK-XXII/2 expedition to the Arctic Ocean from 28 July to 7 October in 2007 on board R/V *Polarstern*. The ARK-XXII/2 expedition was carried out in the context of the International Polar Year-GEOTRACES program, which aims to better understand the cycling of trace elements and isotopes in the oceans. In this expedition, the sea ice edge was first met at ~81°N in Transect 1 (Figure 1), which ended under heavy ice conditions over the Eurasian Basin. Transect 2 was completely ice covered. Transect 3 was also ice covered, but during the return, we very often saw melting sea ice and open water. In Transect 4, the sea-ice edge was located at ~83°N. Down south, the transect was largely in open water. A map showing the sea-ice distribution during this expedition is available online at http://epic.awi.de/Publications/Sch2008ae.pdf. Small-volume (4 L) samples for total ^{234}Th were collected from 12 L Niskin bottles throughout the upper 100–200 m at 36 stations. For each station, a volume of 8 L of seawater was collected at 100 m in order to determine the POC/^{234}Th ratio on >1.0 μm size class particles. At selected stations, large-volume (200–1000 L) seawater was also sampled from 100 m depth using in situ pumps (Challenger Oceanic) equipped with 142 mm diameter filtration holders. Seawater was pumped at a flow rate of up to ~8 L min^{-1} sequentially through a 100 μm Nitex screen, a 53 μm Nitex screen, a 1.0 μm (nominal pore size) quartz microfiber filter (QMA, Whatman), and two 10 inch MnO_2-impregnated cartridges. After sample collection, particles on the 100 and 53 μm pore size Nitex screens were resuspended by ultrasonication in filtered seawater and recollected on 47 mm 1.0 μm QMA filters. The 142 mm QMA filters as well as the 47 mm QMA filters were dried overnight, and a 22 mm subsample was cut from each filter and prepared for beta counting.

2.2. Thorium-234 Analyses

[6] Analysis for total ^{234}Th in 4 L samples was based on the small-volume MnO_2 coprecipitation method with addition of a ^{230}Th spike [*Buesseler et al.*, 2001; *Pike et al.*,

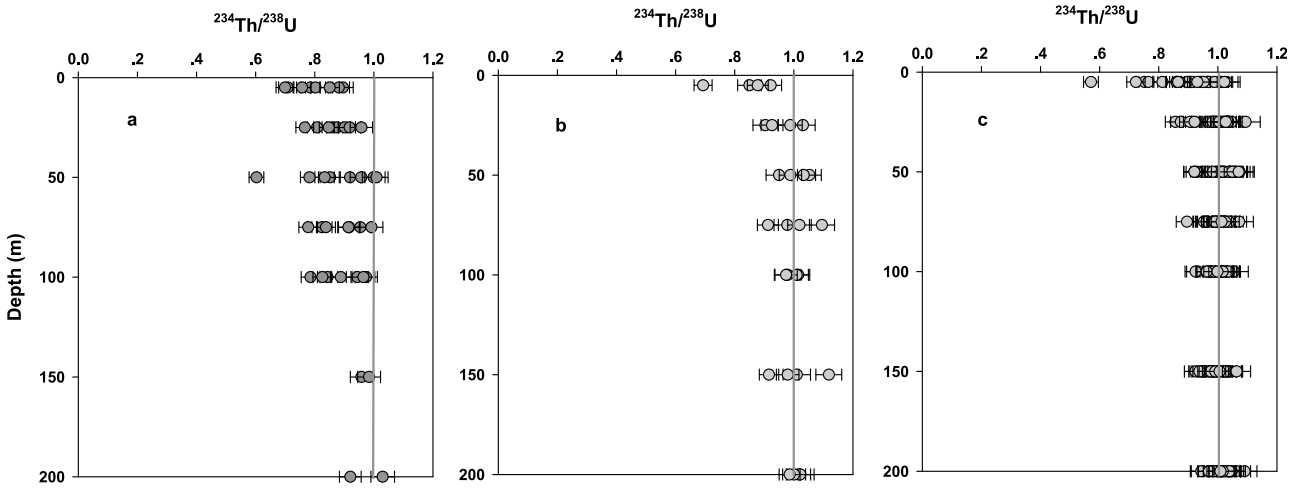

Figure 2. Depth profiles of total $^{234}Th/^{238}U$ over the (a) shelf, (b) slope, and (c) deep basin of the Arctic Ocean; the filled circles at a same depth refer to samples collected at different stations. The error bar represents 1σ uncertainty associated with the $^{234}Th/^{238}U$ measurements.

2005; *Rutgers van der Loeff et al.*, 2006]. In order to accelerate the filtration speed of MnO_2 suspension onto a 25 mm QMA filter, we have slightly modified the protocol by introducing a heating step immediately after the addition of $KMnO_4$ and $MnCl_2$ solutions [*Cai et al.*, 2006a]. The filtered MnO_2 precipitates were dried, mounted under one layer of Mylar film and one layer of aluminum foil (8.0 mg cm^{-2}), and counted onboard with gas flow proportional beta counters (Risø GM-25-5, Denmark) until the counting uncertainty was below 3%. After 5–6 months, each sample was recounted on a same detector as upon sampling so as to determine the background of other non-$^{234}Th/^{234m}Pa$ beta emitters. About two thirds of the samples were processed for ^{230}Th recovery measurement. Recovery of ^{230}Th onto the MnO_2 precipitate was quantified by inductively coupled plasma–mass spectrometry (ICP-MS) (Element 2, Thermo Finnigan MAT, Germany) with addition of a ^{229}Th internal standard [*Pike et al.*, 2005]. Although there were a few samples with low yields, ^{230}Th recoveries were generally found to be high and stable (94.8% ± 2.4%, n = 152). As indicated in Table A1, for the remaining 84 samples we used the average recovery of 94.8% ± 2.4% to correct the final ^{234}Th activity. Thorium-234 activities were decay-corrected to the time of sampling. The associated errors were propagated from the initial and final counting of ^{234}Th, as well as the uncertainty on the ^{230}Th recovery correction. Uranium-238 activities were estimated from salinity measurements using the relationship of ^{238}U (disintegrations per minute (dpm) L^{-1}) = 0.0713 × salinity [*Pates and Muir*, 2007]. The associated uncertainty is in the vicinity of 3% and was also included when propagating the error related to $^{234}Th/^{238}U$ ratios.

[7] As with total ^{234}Th in seawater, particulate samples were beta counted for initial ^{234}Th activities and later for final background. Detector calibration for the total and particulate ^{234}Th samples was conducted using aged seawater as described by *Cai et al.* [2006b]. As a check, deep water samples (>1000 m) were analyzed in a Southern Ocean cruise, and they showed a $^{234}Th/^{238}U$ ratio of 1.00 ± 0.04 (n = 5) (M. Rutgers van der Loeff et al., ^{234}Th in surface waters: Distribution of particle export flux across the Antarctic Circumpolar Current and in the Weddell Sea during the GEOTRACES expedition ZERO and Drake, submitted to *Deep Sea Research*, *Part II*, 2010).

2.3. POC and Chlorophyll *a* Measurements

[8] After beta counting, the particulate samples were then used to determine POC concentration. POC concentrations were determined with a Eurovector C/N element analyzer (Euroanalysator EA) according to the Joint Global Ocean Flux Study (JGOFS) protocols [*Knap et al.*, 1994, 1996]. All samples were treated with 0.1 *M* HCl solution to remove the carbonate. Each sample was corrected for a C blank. The C blank of the filter was less than 15 μg C, which is generally <10% of the POC on the QMA filters. On the basis of replicate analyses, the precision for the POC determination was <5%.

[9] The chlorophyll *a* (Chl *a*) data presented in this study was derived from fluorometer readout of chlorophyll fluorescence. In order to convert the flow-through fluorescence to Chl *a* concentration, discrete seawater samples were collected from Niskin bottles and about 0.5–2.0 L of seawater was filtered through Whatman GF/F filters and stored at −18°C. At the Alfred-Wegener Institute for Polar and Marine Research, the filters were extracted in 90% acetone and analyzed with a spectrophotometer for higher values and with a Turner Design fluorometer for lower values. The relationship between the measured Chl *a* and the flow-through fluorescence was Chl *a* = 1.33 × fluorescence (R^2 = 0.814, n = 63).

3. Results

3.1. Depth Distributions and Spatial Variability of Total ^{234}Th

[10] The total ^{234}Th data here presented (see Table A1) are available on line at http://doi.pangaea.de/10.1594/PANGAEA.712155. For comparison purposes, the depth profiles of total ^{234}Th were classified into three categories in terms of water depth of the sampling stations, i.e., shelf

(<300 m), slope (>300–1000 m), and deep basin (>1000 m, hereafter also referred to as the central Arctic Ocean) stations (Figure 2). Strikingly, ^{234}Th deficit with respect to ^{238}U in the upper 100 m was significant only over the shelf regions. The largest ^{234}Th deficit occurred at the innermost station in the Laptev Sea (Figure 1), where the ^{234}Th/^{238}U ratio at 50 m was ~0.60. Meanwhile, it should be noted that the water depth at this station is only 72 m. As such, it seems that the large ^{234}Th deficit at 50 m was more likely a signal of sediment resuspension rather than a signal of export of in situ-produced particles. For the other shelf stations, the ^{234}Th/^{238}U ratio in the upper 100 m varied between 0.70 and 1.00 (Figure 2a). In contrast, the ^{234}Th/^{238}U ratio was very close to unity over both the slope and deep basin regions (Figures 2b and 2c). In fact, for the 30 depth profiles over the slope and deep basin regions, the average ^{234}Th/^{238}U ratios at 5, 25, 50, 75, 100, 150, and 200 m were 0.89 ± 0.11, 0.99 ± 0.06, 1.01 ± 0.05, 1.00 ± 0.04, 1.00 ± 0.03, 1.00 ± 0.04, and 1.01 ± 0.03, respectively. The associated error is one standard deviation for the 30 measurements at different stations, which reflects the horizontal variability in total ^{234}Th activities. It is evident that ^{234}Th deficit occurred only at the surface, and likely at 25 m in at least a few cases. Below 25 m, ^{234}Th/^{238}U ratios were essentially undistinguishable from 1. In addition, the one standard deviation confirmed the uncertainty associated with an individual measurement of the ^{234}Th/^{238}U ratio (±3%–5%). This indicates that over the slope and deep basin of the Arctic Ocean, ^{234}Th removal and particle export below 25 m was very small.

[11] In order to examine the spatial variability of total ^{234}Th in more detail, we have plotted the contours of the ^{234}Th/^{238}U ratio versus depth along the shelf slope-deep-basin transects (Figures 3, 4, 5, and 6). All data were processed using a software package (Ocean Data View 3.4.1), which utilizes a VG gridding algorithm to grid the data. In the application of the algorithm, the average length scales for the *x* and *y* axis were generally set to be 200 or 250 per mille of the full axis range. Transect 1 comprised nine stations, four of which were located in the Barents Sea. Two stations were occupied over the continental slope and the other three extended to the deep Eurasian Basin (Figure 3). In the Barents Sea, where the bottom depth is generally in the range of 150–300 m, a ^{234}Th deficit was observed throughout the upper 100 m. Here, the chlorophyll concentration was also found to be much higher than in the deep basin. Higher chlorophyll concentrations indicate increased phytoplankton biomass and enhanced particle production rates through primary production. This suggests enhanced particle production and export rates in the Barents Sea, which occurred in the course of the receding ice edge toward the north [*Comiso et al.*, 2008]. Over the Eurasian basin, aside from low chlorophyll concentration, ^{234}Th/^{238}U ratios were very close to unity, indicating low particle export in this regime. Another interesting feature of Transect 1 was the low surface ^{234}Th associated with a low-salinity plume at the continental shelf edge between 81°N and 82°N (Figure 3). This low-salinity plume was located roughly at the edge of the perennial Arctic sea ice cover, and therefore was believed to be a result of freshwater input from sea ice melting. During sea ice melting, ice algae may have been released, and an ice edge bloom might be triggered, thereby resulting in enhanced particle export and hence the low observed ^{234}Th activities. Coincidently, surface nitrate was found to be depleted (plot not shown) and a large deficit of biogenic barium (up to 20%–40%) was observed in the low-salinity plume (T. Roeske et al., Utility of dissolved Ba in distinguishing North American from Eurasian runoff and in characterizing processes in surface waters of the Arctic Ocean, manuscript in preparation, 2010), in support of the notion of an ice edge bloom.

[12] Transect 2 consisted of five stations: two on the continental slope of the Barents Sea and three in the deep Eurasian Basin (Figure 4). In this transect, ^{234}Th deficit was confined to the upper 25 m, where salinity was relatively low and chlorophyll concentration was relatively high. Below 25 m, the chlorophyll concentration was low and the ^{234}Th deficit was generally absent, indicating low biological productivity and low POC export in the central Arctic Ocean.

[13] Transect 3 included 11 stations (Figure 5). It started from the Kara Sea shelf edge, crossed the whole Eurasian Basin, extended onto the Makarov Basin, a subbasin of the Canadian Basin, and passed the Alpha Ridge (Figure 1). In this transect, we saw the intrusion of a low-salinity plume from the Canadian Basin into the Eurasian Basin. This low-salinity plume has been documented in previous studies. The Pacific water flows in through the Bering Strait over the Siberian shelves and mixes with the freshwater input from Siberian rivers, thereby creating a low-salinity lens in the central Arctic Ocean [e.g., *Anderson et al.*, 1994]. Meanwhile, a slight ^{234}Th deficit was observed only over the Kara Sea shelf edge and the Eurasian Basin, and the deficit was again confined to the upper 25 m. From Figure 5, we can see that there was no direct correlation between ^{234}Th deficit and the freshwater lens. Nonetheless, the ^{234}Th deficit was associated closely with enhanced chlorophyll concentrations. This suggests that in situ production and export of biogenic particles are the main mechanism for ^{234}Th removal in the surface of the central Arctic Ocean.

[14] Transect 4 was composed of eight stations, which covered the Eurasian Basin and extended into the Laptev Sea shelf (Figure 6). Over the Laptev Sea shelf, ^{234}Th was found to be in deficit with respect to ^{238}U throughout the whole water column. The largest ^{234}Th deficit occurred at the innermost station in the Laptev Sea, and could be partly caused by the resuspension of bottom sediments as the bottom depth at this station is only a few tens of meters. In this transect, surface ^{234}Th deficit was found to be coupled with a freshwater lens. Chlorophyll concentrations at the shelf edge were the highest values (up to 2.4 μg L^{-1}) measured during the cruise, indicating an ongoing plankton bloom in the freshwater lens. Concurrently, dissolved barium was also depleted in the freshwater lens over the Laptev Sea shelf, indicating enhanced biological activity herein (T. Roeske et al., manuscript in preparation).

[15] Taken together, the overall feature of the ^{234}Th distribution in the central Arctic Ocean is that the ^{234}Th deficit was confined to the upper 25 m. Moreover, the surface ^{234}Th deficit was generally found to be associated with enhanced chlorophyll concentration, indicating that in situ production and export of biogenic particles are the main mechanism for surface ^{234}Th removal. Enhanced subsurface ^{234}Th removal was observed over the Arctic shelves, pos-

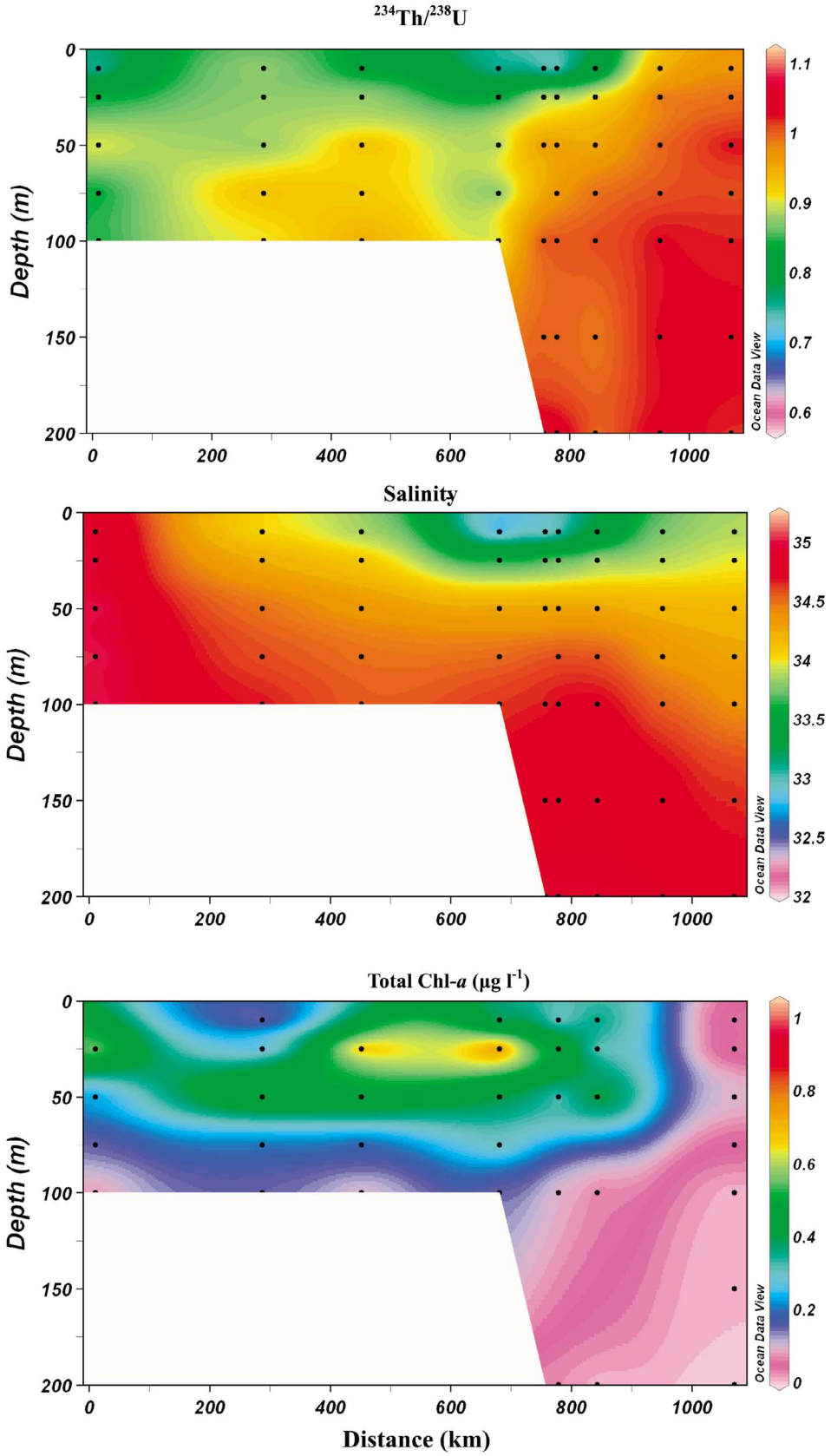

Figure 3. Total $^{234}Th/^{238}U$ ratio, salinity, and total Chl *a* in the upper 200 m along Transect 1.

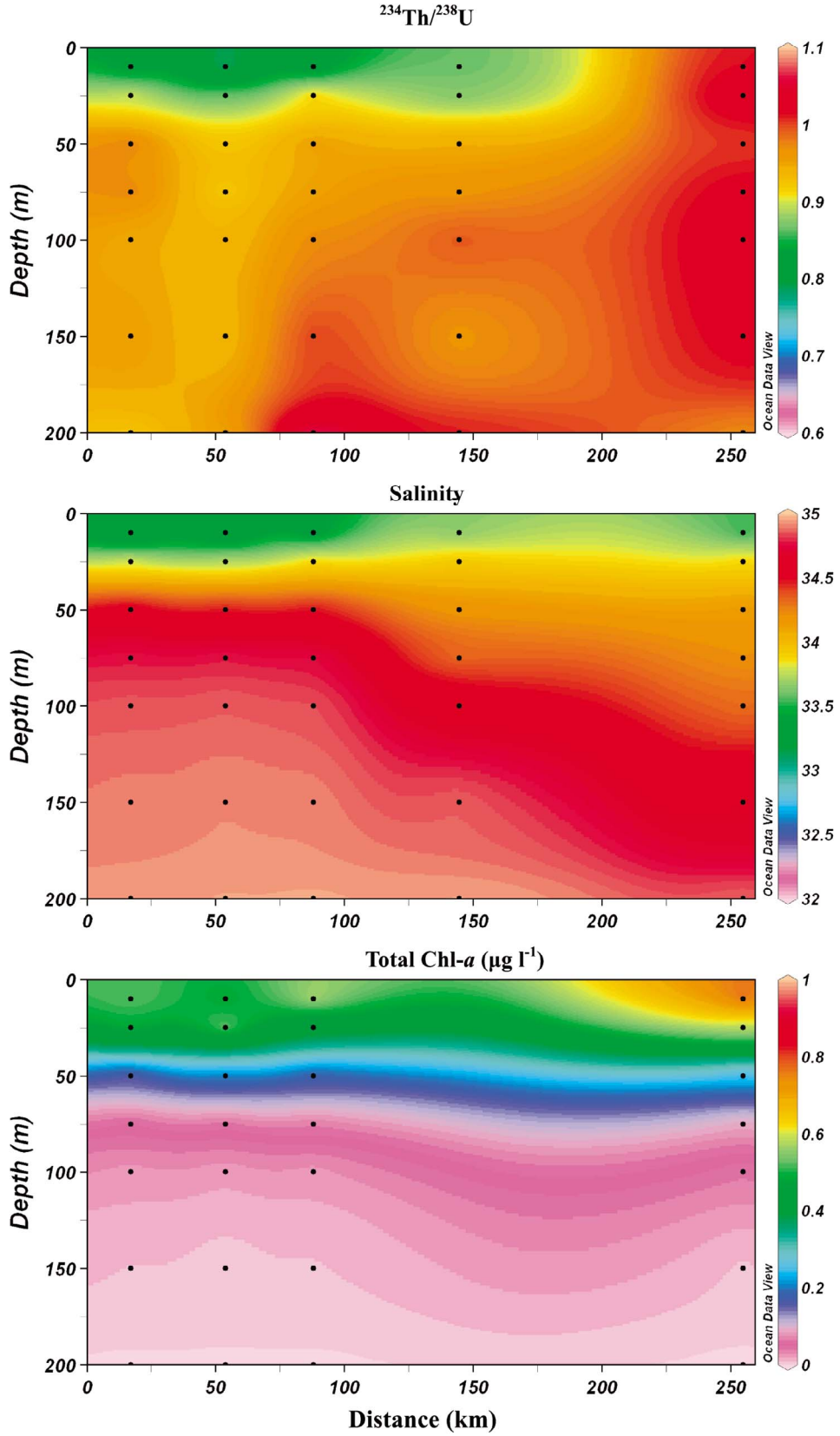

Figure 4. Total $^{234}Th/^{238}U$ ratio, salinity, and total Chl *a* in the upper 200 m along Transect 2.

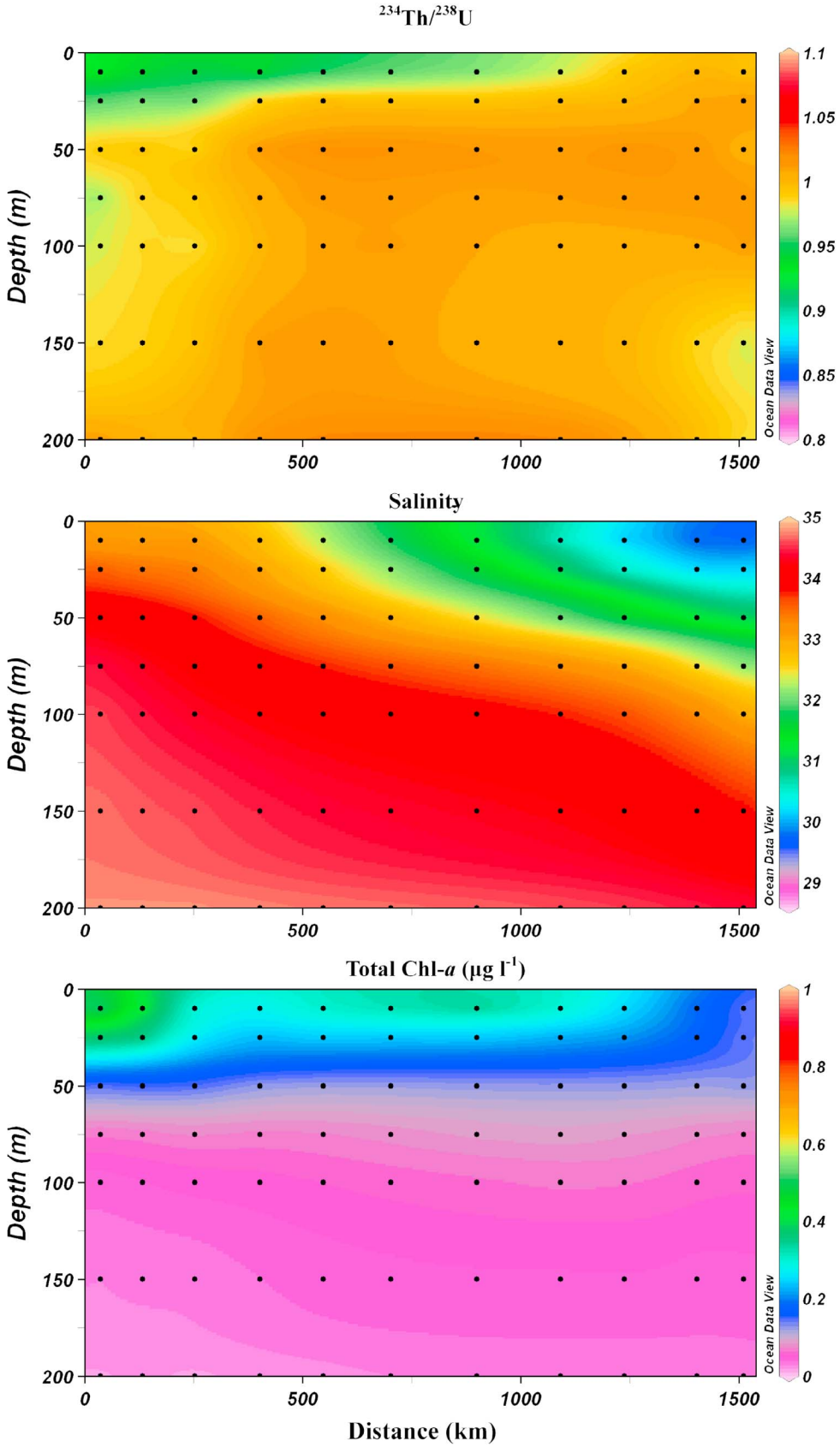

Figure 5. Total $^{234}Th/^{238}U$ ratio, salinity, and total Chl *a* in the upper 200 m along Transect 3.

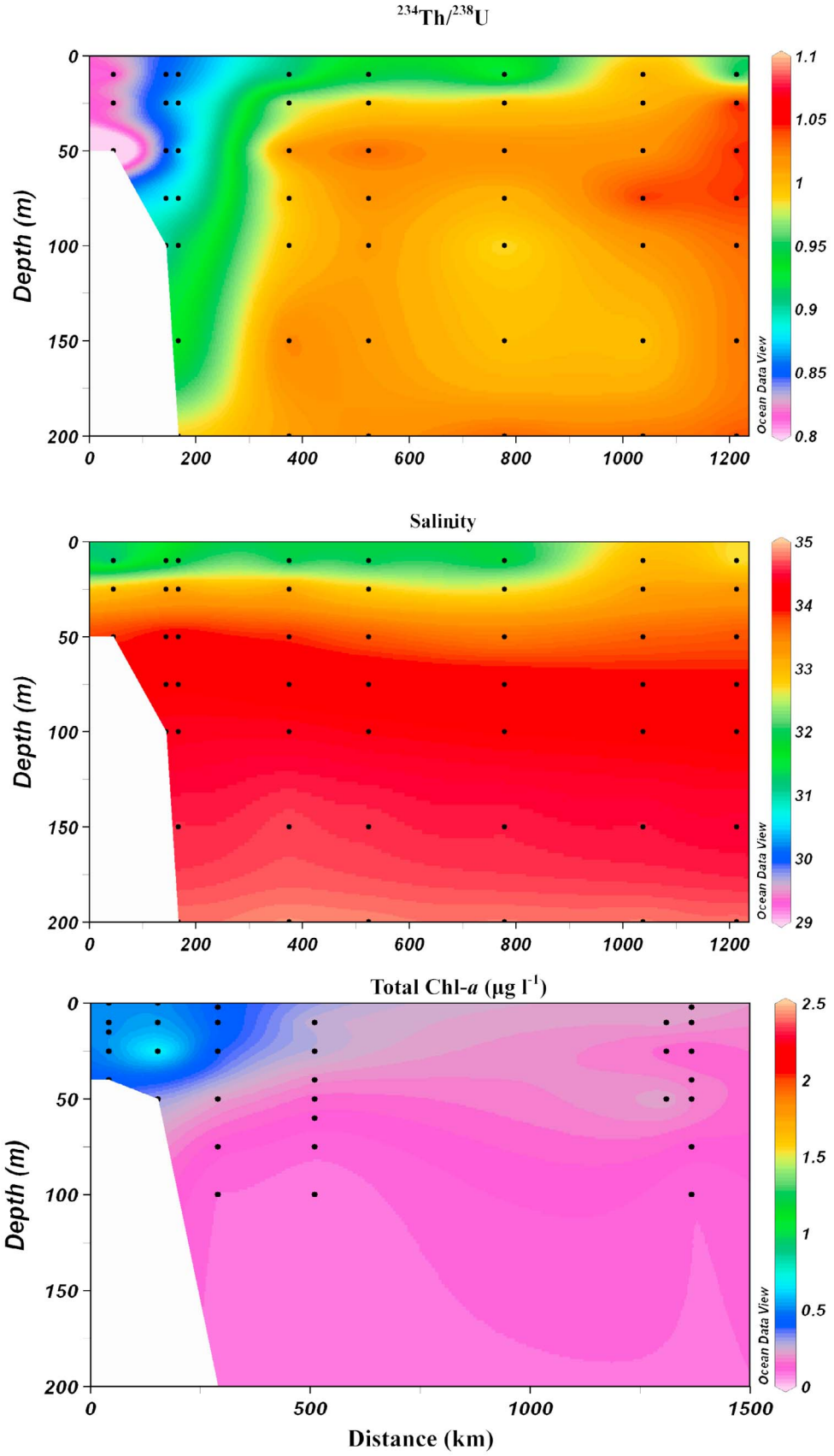

Figure 6. Total $^{234}Th/^{238}U$ ratio, salinity, and total Chl *a* in the upper 200 m along Transect 4.

sibly due to a combination of elevated biological productivity and the resuspension of bottom sediments.

3.2. Particulate ^{234}Th Activities

[16] At the export horizon (50 or 100 m), particulate ^{234}Th activities ranged from a low of 0.14 ± 0.01 dpm L^{-1} to a high of 1.27 ± 0.03 dpm L^{-1} on total suspended particles collected by Niskin bottles and were generally found to be enhanced over the shelf areas (Table A2). The activities of size-fractionated particulate ^{234}Th varied between 0.06 ± 0.003 dpm L^{-1} and 0.45 ± 0.01 dpm L^{-1} on small (<53 μm) particles collected on 1 μm QMA filters. The activities of ^{234}Th on 53–100 μm and >100 μm particles collected on Nitex screens were very low, ranging between 0.001 ± 0.001 dpm L^{-1} and 0.070 ± 0.002 dpm L^{-1}. On average, ^{234}Th activities on medium- and large-size particles each accounted for only ~5% of the total particulate ^{234}Th activity collected via in situ pumping. Similar to particulate ^{234}Th on total suspended particles, size-fractionated particulate ^{234}Th generally had elevated activities over the shelf regions.

[17] It is important, however, to note that the total particulate thorium activity calculated as the sum of size-fractionated activities (pump Th) was remarkably lower than the particulate thorium activity on total suspended particles collected by Niskin bottles (bottle Th). In this case, the pump ^{234}Th/bottle ^{234}Th ratios ranged from 0.35 to 0.84, with an average of 0.58 ± 0.16 (1 standard deviation, n = 11). This observation is in conflict with an earlier study, which showed no significant difference in pump versus bottle particulate ^{234}Th activities [*Cai et al.*, 2006b]. The mechanisms of this discrepancy remain unclear and need to be further investigated. A possible explanation is that the two studies used different pump inlet designs, while a more recent study [*Liu et al.*, 2009] has demonstrated that inlet design can affect the efficiency and retention of large particles (and hence particulate ^{234}Th) on pump filters.

3.3. Particulate Organic Carbon

[18] At the export horizon, POC concentrations collected via Niskin bottles (bottle POC) ranged from 0.8 μmol L^{-1} to 7.5 μmol L^{-1}. High POC concentrations were observed over the shelf regions, possibly due to increase in particle loads caused by a combination of enhanced biological productivity and sediment resuspension. Size-fractionated POC concentrations ranged from 0.19 μmol L^{-1} to 1.9 μmol L^{-1} on small particles (1–53 μm). In comparison, POC concentrations measured on medium- (53–100 μm) and large- (>100 μm) size particles ranged from 0.006 μmol L^{-1} to 0.44 μmol L^{-1} and from 0.009 μmol L^{-1} to 0.72 μmol L^{-1}, respectively (Table A2). On average, POC concentrations measured on medium and large particles accounted for 8.6% and 6.5% of the total pump POC, respectively. Similar to bottle POC, enhanced concentrations of size-fractionated POC were observed over the shelf regions.

[19] As with particulate ^{234}Th activities, pump POC concentrations were found to be considerably lower than bottle POC concentrations. The pump POC/bottle POC ratios ranged from 0.18 to 0.51, with an average of 0.33 ± 0.11 (1 standard deviation, n = 11). Low pump POC relative to bottle POC has often been observed in previous studies, and a number of factors have been proposed to explain the discrepancy. These include higher pressure in pumps, dissolved organic carbon (DOC) absorption onto filters, use of different filter types in pump filtration versus bottle filtration, contamination during bottle filtration, particle washout during pump recovery, and preferential capture of living zooplankton by Niskin bottles [*Liu et al.*, 2005]. *Liu et al.* [2009] further demonstrated that different inlet design can affect the efficiency and retention of particles on pump filters. Thus, causes of the discrepancy between pump POC and bottle POC seem to be complex, and further investigations are needed to resolve this issue.

4. Discussion

4.1. Thorium-234 Export Fluxes

[20] Export fluxes of ^{234}Th on sinking particles can be determined by solving for the balance of its supply and removal rates with the following mathematical expression:

$$\partial A/\partial t = (A_p - A) \cdot \lambda - P + V \quad (1)$$

where $\partial A/\partial t$ is the change in ^{234}Th activity with time, A_p is the activity of ^{238}U, A is the activity of total ^{234}Th, λ is the decay constant for ^{234}Th (= 0.0288 d^{-1}), P is the net export flux of ^{234}Th on sinking particles, and V is the sum of advective and diffusive terms. In the open ocean, the magnitude in P is determined mostly by the extent of the disequilibrium between ^{234}Th and ^{238}U. Advective and diffusive terms are generally ignored, and steady state (SS) is often assumed [*Savoye et al.*, 2006].

[21] The V term in equation (1) includes horizontal and vertical advective and diffusive processes. Horizontal ^{234}Th transport can be important in coastal regions, especially in bays, where large horizontal gradients in ^{234}Th scavenging can occur [e.g., *Benitez-Nelson et al.*, 2000; *Charette et al.*, 2001]. Vertical transport, meanwhile, has been demonstrated to be significant in areas of intense upwelling and in mesoscale cold-core eddies [e.g., *Buesseler et al.*, 1995; *Maiti et al.*, 2008]. The significance of horizontal transport in the calculation of ^{234}Th fluxes depends essentially on two terms: the magnitudes of advection velocity and eddy diffusivity and the activity gradient of ^{234}Th. To evaluate the significance of horizontal transport in the overall ^{234}Th balance, we can make a comparison between the Arctic Ocean and the South China Sea, the second largest marginal sea in the world. In the South China Sea, the total ^{234}Th activities varied from a low of 1.54 ± 0.09 dpm L^{-1} to a high of 3.44 ± 0.16 dpm L^{-1}, and horizontal transport has been demonstrated to contribute <10% of the overall ^{234}Th balance [*Cai et al.*, 2008a]. In comparison, total ^{234}Th activities in the Arctic Ocean varied in a narrower range, between 1.33 ± 0.04 dpm L^{-1} and 2.79 ± 0.04 dpm L^{-1} (Table A1). Taking further into account the larger length scale, we expect to see a much smaller gradient of total ^{234}Th in the Arctic Ocean. Eddy diffusivity calculation, however, suggested that the horizontal diffusivity in the central Arctic Ocean was comparable to that in the South China Sea [*Huang et al.*, 1997; *Moran et al.*, 1997]. As such, we assume that the horizontal transport was negligible in the overall ^{234}Th balance.

[22] Significance of the vertical transport term in the overall ^{234}Th balance can be assessed if the vertical diffusivity and ^{234}Th activity gradient are known. Vertical eddy

diffusivity was low (0.17 m^2 d^{-1}) in the Arctic Ocean [*Wallace et al.*, 1987], presumably because of the strong density stratification caused by the freshwater lens over the large parts of the Arctic Ocean. In the present study, the maximum ^{234}Th deficit in the upper 100 m was observed at station PS70-239 in the Barents Sea (Table A1). To estimate an upper limit of ^{234}Th gradient, we assumed that total ^{234}Th below 100 m at this location was in secular equilibrium with ^{238}U. Despite that this assumption may not be valid as the bottom depth is only 214 m and hence lower ^{234}Th activity than seawater ^{238}U is expected because of the scavenging of resuspended sediment, we derived a maximum ^{234}Th gradient of 0.58 dpm L^{-1} over half the depth of the region of ^{234}Th deficit (approximately 50 m). Multiplying this gradient by the vertical eddy diffusivity of *Wallace et al.* [1987] gives an upper limit of ~1.0 dpm m^{-2} d^{-1} for the upward diffusive flux of ^{234}Th. This term was too small to consider when compared to the overall uncertainty associated with the ^{234}Th flux model. Therefore, we neglected the vertical transport term when calculating the export fluxes of ^{234}Th.

[23] The use of NSS (non-steady state) ^{234}Th formulations in equation (1) appears to be important during plankton blooms, when significant ^{234}Th removal can occur [e.g., *Buesseler et al.*, 1998]. SS models are generally considered sufficient, however, when SS ^{234}Th fluxes are low, i.e., <800 dpm m^{-2} d^{-1} (for review see *Savoye et al.* [2006]). As will be shown below, most of the SS ^{234}Th fluxes from the upper 100 m in this study were below this value. Meanwhile, there are a few stations over the shelf regions which displayed SS ^{234}Th fluxes >800 dpm m^{-2} d^{-1}. For these stations, it is somewhat difficult to assess the SS assumption as time series sampling was not conducted during this cruise. In this case, we also neglected the NSS term in the ^{234}Th flux calculations, i.e., assuming $\partial A/\partial t = 0$.

[24] With these simplifications, equation (1) takes the form

$$P = \left(A_p - A\right) \cdot \lambda. \tag{2}$$

From the integral disequilibrium between parent-daughter nuclides, P (in terms of dpm m^{-2} d^{-1}) can be solved for the depth horizon of interest. Results for the flux calculation are listed in Table 1. The export fluxes of ^{234}Th in the upper Arctic Ocean ranged from -281 ± 126 dpm m^{-2} d^{-1} to 1458 ± 99 dpm m^{-2} d^{-1}, and nearly half the stations were characterized by a negative ^{234}Th flux. Meanwhile, most of the negative fluxes were relatively small, ranging between -2 ± 118 dpm m^{-2} d^{-1} and -281 ± 126 dpm m^{-2} d^{-1}. Given total errors on ^{234}Th of 3%–5% and five independent measurements that were evenly spaced over the upper 100 m, we estimate the $\pm 1\sigma$ uncertainty associated with the calculated ^{234}Th fluxes at 100 m to be around ± 120 dpm m^{-2} d^{-1}. In this regard, all of the negative values listed in Table 1 were within the range of $\pm 2.58\sigma$ uncertainty ($p = 0.99$) of the calculated ^{234}Th fluxes, indicating that the negative fluxes were most likely caused by the errors associated with total ^{234}Th measurements. In fact, if we use the definition

$$\mathrm{MDL} = 3\sigma \tag{3}$$

where MDL is the "minimum detection limit" of the ^{234}Th method, then we derive a below-detection ^{234}Th flux threshold of ~360 dpm m^{-2} d^{-1}. From Table 1, we can see that most of the ^{234}Th fluxes in the basin region were below this threshold. This suggests that the central Arctic Ocean is an environment with very low particle flux and that the ^{234}Th method is close to its limit in determining POC export in such environments.

[25] Figure 7 shows the geographic distribution of ^{234}Th export fluxes in the upper Arctic Ocean. Relatively high export fluxes were generally observed in the coastal seas, i.e., in the Barents Sea, Kara Sea, and Laptev Sea, indicating enhanced particle production and removal rates over the Arctic shelves. In comparison, ^{234}Th export fluxes were low and uniform in the basin regions. The low ^{234}Th export fluxes are consistent with previous observations of negligible ^{234}Th export in the ice-covered northern Fram Strait [*Rutgers van der Loeff et al.*, 2002] and are a reflection of weak particle production and removal in the central Arctic Ocean. The geographic pattern of ^{234}Th export fluxes was also consistent with the distribution of the depletion of biogenic barium, which revealed enhanced biological activity over the Arctic shelves (T. Roeske et al., manuscript in preparation).

4.2. POC/^{234}Th Ratio

[26] If the flux of ^{234}Th on sinking particles is known, then the export flux of POC can be estimated from the knowledge of the ratio of POC to ^{234}Th on particles by

$$\mathrm{POC\ flux} = {}^{234}\mathrm{Th\ flux} \cdot \mathrm{POC}/{}^{234}\mathrm{Th}. \tag{4}$$

This approach assumes that we know the flux of ^{234}Th accurately and that the POC/^{234}Th ratio is representative of sinking particles at the depth horizon of interest [*Buesseler et al.*, 1992]. Prior studies have shown that POC/^{234}Th ratios may vary by as much as three orders of magnitude, and the mechanisms for the variation have recently been reviewed [*Buesseler et al.*, 2006]. In brief, variations in POC/^{234}Th ratio can result from a variety of geochemical and biological processes, such as changes in volume:surface area ratio, particle aggregation/disaggregation, preferential assimilation and degradation of POC on sinking particles, shifts in particle type, and alterations in solution chemistry associated with complexation of ^{234}Th. In addition, simple decay of ^{234}Th may also play a role [*Cai et al.*, 2006c].

[27] In the present study, for each station we have measured the POC/^{234}Th ratio on total suspended particles from the export horizon. The results are listed in Table 1. As large-size particles are thought to be more representative for sinking material, POC/^{234}Th ratio on >53 μm particles was generally used to convert ^{234}Th fluxes into POC export rates. Unfortunately, in the present study, because of the lack of ship time, in situ pumps were deployed only at selected stations to collect large-size particles. To uniform data, we have compared the POC/^{234}Th ratios on total suspended particles and on >53 μm size particles (which include those retained in the >100 μm fraction) collected at these stations. As shown in Figure 8, except for two stations, POC/^{234}Th ratios on total suspended particles collected by Niskin bottles (bottle POC/^{234}Th) were slightly higher than on >53 μm size particles collected via in situ pumping (pump POC/^{234}Th). The two notable exceptions occurred at station PS70-239 and PS70-260, where pump POC/^{234}Th

Table 1. Thorium-234 Fluxes, POC/^{234}Th Ratios, and POC Export in the Upper Arctic Ocean

Station PS70-	Latitude (N)	Longitude (E)	Export Horizon (m)	Thorium-234 Flux (dpm m^{-2}d^{-1})	POC/^{234}Th$_b$[a] (μmol dpm^{-1})	POC/^{234}Th$_n$[b] (μmol dpm^{-1})	POC Flux[c] (mmol m^{-2}d^{-1})
228	75° 00.058′	34° 00.090′	100 m	1115 ± 107	6.4 ± 0.4	4.9 ± 1.0	5.5 ± 1.2
236	77° 30.040′	33° 58.390′	100 m	753 ± 104	6.3 ± 0.3	4.8 ± 0.9	3.6± 0.9
237	78° 59.790′	33° 58.270′	100 m	603 ± 106	3.7 ± 0.1	2.8 ± 0.5	1.7 ± 0.4
239	81° 00.306′	34° 03.055′	100 m	1458 ± 99	2.5 ± 0.1	1.9 ± 0.4	2.8 ± 0.6
243	81° 43.804′	33° 59.552′	100 m	−107 ± 137	5.4 ± 0.3	4.1 ± 0.8	−0.4 ± 0.6
246	81° 52.715′	34° 01.369′	100 m	662 ± 104	3.6 ± 0.1	2.8 ± 0.5	1.8 ± 0.4
255	82° 30.848′	33° 55.247′	100 m	347 ± 109	3.9 ± 0.2	3.0 ± 0.6	1.0 ± 0.4
257	83° 29.861′	34° 02.595′	100 m	−89 ± 126	5.1 ± 0.5	3.9 ± 0.8	−0.3 ± 0.5
260	84° 30.099′	36° 05.015′	100 m	−56 ± 127	4.2 ± 0.2	3.2 ± 0.6	−0.2 ± 0.4
261	84° 38.720′	60° 56.020′	100 m	−142 ± 110	5.6 ± 0.3	4.3 ± 0.8	−0.6 ± 0.5
264	83° 38.502′	60° 25.723′	100 m	518 ± 107	6.0 ± 0.3	4.6 ± 0.9	2.4 ± 0.7
266	83° 07.643′	61° 48.491′	100 m	413 ± 108	3.2 ± 0.2	2.5 ± 0.5	1.0 ± 0.3
268	82° 48.370′	60° 47.820′	100 m	838 ± 105	3.8 ± 0.1	2.9 ± 0.5	2.4 ± 0.6
271	82° 30.180′	60° 47.710′	100 m	375 ± 108	4.7 ± 0.2	3.6 ± 0.7	1.4 ± 0.5
276	82° 05.091′	68° 57.169′	100 m	438 ± 121	3.0 ± 0.2	2.3 ± 0.4	1.0 ± 0.3
279	81° 13.808′	86°10.759′	100 m	341 ± 109	3.3 ± 0.2	2.6 ± 0.5	1.1 ± 0.4
285	82°08.500′	86° 19.850′	100 m	−15 ± 110	5.4 ± 0.2	4.2 ± 0.8	−0.1 ± 0.5
295	83° 16.330′	86° 17.030′	100 m	488 ± 105	5.5 ± 2.1	4.2 ± 1.8	2.1 ± 1.0
301	84°33.645′	89° 48.780′	100 m	−77 ± 124	10.1 ± 0.6	7.8 ± 1.5	−0.6 ± 1.0
306	85° 55.370′	91° 07.330′	100 m	−281 ± 126	1.7 ± 0.1	1.3 ± 0.3	−0.4 ± 0.2
309	87° 02.554′	104° 55.831′	100 m	−123 ± 108	5.1 ± 0.3	3.9 ± 0.8	−0.5 ± 0.4
316	88° 10.620′	139° 36.980′	100 m	92 ± 106	5.6 ± 0.3	4.3 ± 0.8	0.4 ± 0.5
328	87° 49.295′	−170° 18.573′	100 m	−2 ± 118	7.9 ± 0.4	6.1 ± 1.2	0.0 ± 0.7
333	88°10.620′	−139° 36.980′	100 m	−127 ± 112	8.4 ± 0.4	6.4 ± 1.2	−0.8 ± 0.7
338	85° 42.084′	−135° 01.570′	100 m	−136 ± 100	4.4 ± 0.2	3.4 ± 0.6	−0.5 ± 0.3
342	84° 29.936′	−138° 24.019′	100 m	−45 ± 96	6.3 ± 0.3	4.8 ± 0.9	−0.2 ± 0.5
349	85° 04.275′	−164° 32.311′	100 m	−151 ± 117	5.0 ± 0.3	3.9 ± 0.8	−0.6 ± 0.5
352	86° 38.688′	177° 33.764′	100 m	−90 ± 119	5.8 ± 0.4	4.5 ± 0.9	−0.4 ± 0.5
358	86° 30.228′	151° 58.641′	100 m	169 ± 104	9.5 ± 0.5	7.3 ± 1.4	1.2 ± 0.8
371	84° 39.200′	102° 44.180′	100 m	−178 ± 124	5.9 ± 0.3	4.6 ± 0.9	−0.8 ± 0.6
379	82° 11.699′	119° 33.653′	100 m	84 ± 103	7.8 ± 0.4	6.0 ± 1.2	0.5 ± 0.6
383	80° 39.570′	122° 13.411′	100 m	−127 ± 124	9.1 ± 0.5	7.0 ± 1.4	−0.9 ± 0.9
385	79° 20.778′	124° 20.777′	100 m	−83 ± 125	6.4 ± 0.3	4.9 ± 0.9	−0.4 ± 0.6
400	77° 22.177′	123° 24.896′	100 m	426 ± 106	2.1 ± 0.1	1.6 ± 0.3	0.7 ± 0.2
403	77° 08.995′	123° 07.458′	100 m	1200 ± 98	1.8 ± 0.1	1.4 ± 0.3	1.6 ± 0.3
407	76° 10.876′	122° 08.448′	50 m	928 ± 65	5.9 ± 0.2	4.6 ± 0.9	4.2 ± 0.8

[a]POC/^{234}Th ratio measured on total suspended particles collected by Niskin bottles.
[b]POC/^{234}Th ratio normalized to pump POC/^{234}Th ratio on >53 μm size class.
[c]POC fluxes <0 were likely the result of the uncertainty associated with total ^{234}Th measurements. These values were maintained in order to derive statistically accurate average of POC export fluxes in the Arctic Ocean.

ratios were up to 13–14 μmol dpm^{-1}, 3–5 times higher than bottle POC/^{234}Th ratios. These ratios were also significantly higher than any of the other pump or bottle POC/^{234}Th ratios. A high POC/^{234}Th ratio on large-size particles has been observed in prior studies and was most often ascribed to the "contamination" by live zooplankton. For instance, *Savoye et al.* [2008] found POC/^{234}Th ratio up to 1100 μmol dpm^{-1} on > 330 μm size particles at 130 m during the Southern Ocean Kerguelen Ocean and Plateau compared Study (KEOPS) experiment. *Buesseler et al.* [2009] reported POC/^{234}Th ratios of >50–200 μmol dpm^{-1} on >51 μm size particles below 150 m in the VERtical Transport In the Global Ocean (VERTIGO) program. As zooplankton swimmers are generally characterized by very high POC/^{234}Th ratios [*Rodriguez y Baena et al.*, 2007], even a slight contamination on large-size particles could lead to a high measured POC/^{234}Th ratio. In this study, we did find zooplankton swimmers on >53–100 μm and >100 μm Nitex screens. Although the zooplankton swimmers were hand-picked with the naked eye, slight contamination by small swimmers cannot be ruled out. This might explain the high POC/^{234}Th ratio on large-size particles at station PS70-239 and PS70-260.

[28] As zooplankton swimmers are not considered to be passive sinking material, we therefore excluded these two points and performed a linear regression (with zero intercept) of the remaining data (Figure 8). The results show that the mean ratio of bulk bottle POC/^{234}Th to pump POC/^{234}Th on >53 μm size class was 1.3 ± 0.24. We used this value to normalize the bottle POC/^{234}Th to pump POC/^{234}Th values at each station. The standard error associated with the mean ratio of bottle POC/^{234}Th to pump POC/^{234}Th was propagated during this normalization. The results are listed in Table 1. The normalized ratios varied between 1.3 ± 0.3 μmol dpm^{-1} and 7.8 ± 1.5 μmol dpm^{-1}, and did not show an evident geographic pattern. Our normalized POC/^{234}Th ratios were in general agreement with trap POC/^{234}Th ratios of 3.4–9.2 μmol dpm^{-1} reported in the Barents Sea [*Coppola et al.*, 2002]. Hence, we used these ratios to convert ^{234}Th fluxes into POC export rates.

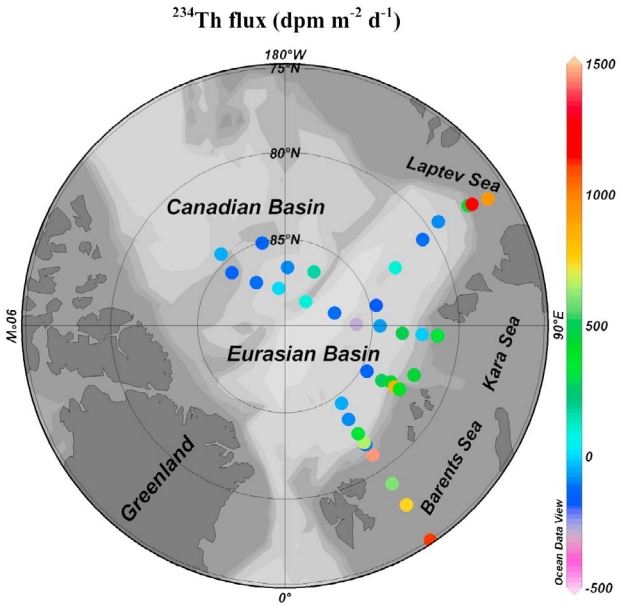

Figure 7. Geographic distribution of ^{234}Th fluxes at 100 m in the Arctic Ocean.

Meanwhile, it should be noted that by applying the normalized POC/^{234}Th ratios, we will derive POC fluxes which are 30% lower than those by directly using the bottle POC/^{234}Th ratios.

4.3. Export Fluxes of Particulate Organic Carbon

[29] As listed in Table 1, POC export fluxes in the upper Arctic Ocean ranged from −0.9 ± 0.9 mmol m^{-2} d^{-1} to 5.5 ± 1.2 mmol m^{-2} d^{-1}, and nearly half the stations were characterized by a negative POC flux. POC export fluxes lower than zero were due to the negative ^{234}Th fluxes that were likely caused by the error associated with total ^{234}Th measurements. As stated above, the MDL, defined as 3σ uncertainty, of ^{234}Th fluxes in this study was ~360 dpm m^{-2} d^{-1}. Multiplying this value by the average "normalized" POC/^{234}Th ratio (4.1 μmol dpm^{-1}, Table 2) gives a below-detection POC export threshold of 1.5 mmol m^{-2} d^{-1} in the Arctic Ocean. From Table 1, we can see that most of the POC export fluxes in the central Arctic Ocean are below this detection threshold, i.e., not resolvable by using the ^{234}Th method. Meanwhile, under the assumption that the error associated with total ^{234}Th measurements was random, we maintained these negative POC fluxes in Table 1 in order to derive a statistically accurate average of POC export fluxes in the Arctic Ocean.

[30] Shown in Figure 9 is the geographic distribution of POC export fluxes in the upper Arctic Ocean. Similar to ^{234}Th fluxes, relatively high POC export was observed over the Arctic shelves. In the central Arctic Ocean, however, POC export fluxes were very low and uniform. More specifically, POC export fluxes in the Barents Sea varied between 1.0 ± 0.4 and 5.5 ± 1.2 mmol m^{-2} d^{-1}, with an average of 2.7 ± 1.7 mmol m^{-2} d^{-1} (1 standard deviation, n = 6). In the Kara Sea and the Laptev Sea, the mean POC export fluxes were 0.5 ± 0.8 mmol m^{-2} d^{-1}(1 standard deviation, n = 2) and 2.9 ± 1.8 mmol m^{-2} d^{-1}(1 standard deviation, n = 2), respectively. In comparison, POC export fluxes in the central Arctic Ocean averaged 0.2 ± 1.0 mmol m^{-2} d^{-1} (1 standard deviation, n = 26). To our knowledge, this is the lowest value ever reported by using ^{234}Th/^{238}U disequilibrium. *Thomalla et al.* [2006] have determined POC export in the Atlantic Ocean by using ^{234}Th/^{238}U disequilibrium. Occasionally, they found POC fluxes equal to zero within uncertainty in the oligotrophic gyres. Meanwhile, the mean POC fluxes over the whole Atlantic gyres in their study were 2.3 ± 2.4 mmol m^{-2} d^{-1} (1 standard deviation, n = 5), higher than our results from the central Arctic Ocean.

[31] There are only a few prior studies of POC export in the central Arctic Ocean using ^{234}Th/^{238}U disequilibrium. The first measurements of ^{234}Th/^{238}U disequilibrium in the interior Arctic were conducted during the 1994 Arctic Ocean Section [*Moran et al.*, 1997]. Evident ^{234}Th deficit with respect to ^{238}U was seen in the upper 200–300 m. From the ^{234}Th/^{238}U disequilibrium and the POC/^{234}Th ratio measured in the 0.7–53 μm particle size class, an average POC flux of 3 ± 2 mmol m^{-2} d^{-1} at the depth horizon of 30 m was determined. In a POC export study of the Beaufort Sea, *Moran and Smith* [2000] collected a depth profile of ^{234}Th in the adjacent Canadian Basin. Evident ^{234}Th deficit with respect to ^{238}U was also seen throughout the upper 150 m, and a POC export flux of 2.4 ± 0.22 mmol m^{-2} d^{-1} at 50 m was determined. *Chen et al.* [2003] have measured a single depth profile of ^{234}Th in the Canadian Basin. From the

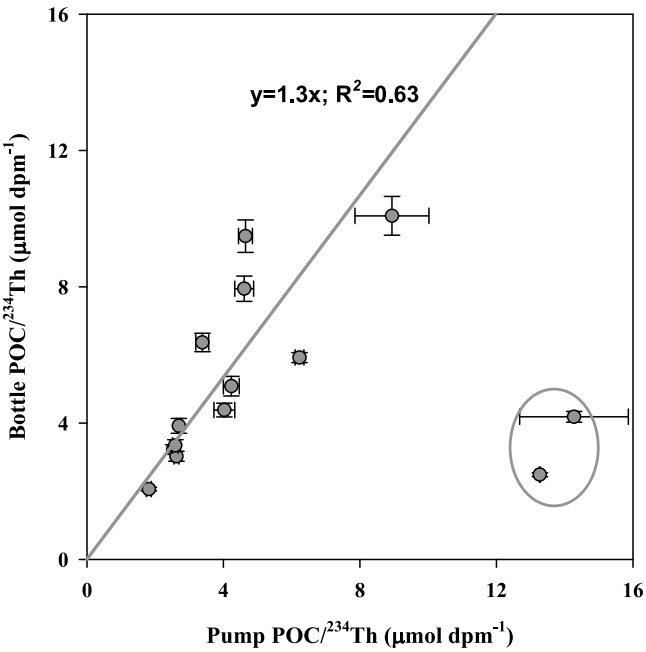

Figure 8. Bottle POC/^{234}Th (not size fractionated) versus pump POC/^{234}Th on >53 μm size class; data points in the ellipse indicate pump samples that were possibly contaminated by swimmers. These data were not included in the regression analysis; the error bar represents 1σ uncertainty associated with the POC/^{234}Th measurements.

Table 2. Comparison of POC/^{234}Th Ratio, ^{234}Th Flux, POC Export, and ThE Ratio Between the Central Arctic Ocean and Other World Oceans

Study Region	Export Depth (m)	POC/^{234}Th (μmol dpm^{-1})	Thorium-234 Flux (dpm m^{-2} d^{-1})	POC Flux[a] (mmol m^{-2} d^{-1})	ThE Ratio[b]	Reference
Central Arctic Ocean	30	5–21	188 ± 141	3 ± 2 (n = 5)	NR	*Moran et al.* [1997]
Central Arctic Ocean (Canadian Basin)	50	8.5	276	2.4 (n = 1)	NR	*Moran and Smith* [2000]
Central Arctic Ocean (Canadian Basin)	100	1.2	824	1 (n = 1)	26%	*Chen et al.* [2003]
Central Arctic Ocean (Canadian Basin)	50	8.3	894	7.4 (n = 1)	NR	*Baskaran et al.* [2003]
Central Arctic Ocean (Canadian Basin)	100	7.4 ± 0.2	354 ± 30	2.6 ± 0.1 (n = 2)	NR	*Trimble and Baskaran* [2005]
Central Arctic Ocean	100	4.1 ± 1.6	85 ± 299	0.2 ± 1.0 (n = 26)	<6%	This study[c]
North Pacific (Station ALOHA)	150	5.9 ± 1.4	765 ± 562	4.0 ± 2.3 (n = 9)	8.8%	*Benitez-Nelson et al.* [2001]
North Pacific	150	1.6 ± 0.3	1092 ± 617	1.8 ± 0.8 (n = 5)	<3%	*Maiti et al.* [2008][d]
North Pacific (Station ALOHA)	150	5.4 ± 1.1	374 ± 394	2.1 ± 2.0 (n = 19)	12%	*Buesseler et al.* [2009]
North Pacific (Station K2)	150	4.0 ± 0.5	1540 ± 524	6.3 ± 2.5 (n = 26)	14%	*Buesseler et al.* [2009][e]
Southern Ocean	100	6.0	653 ± 177	4.0 ± 1.0 (n = 2)	14%	*Buesseler et al.* [2005][f]
Southern Ocean (Zero Meridian)	100	4.5 ± 1.1	1285 ± 365	5.7 ± 2.6 (n = 13)	16%	M. Rutgers van der Loeff et al., submitted manuscript (2010)[g]
Southern Ocean (Drake Passage)	100	4.8 ± 2.2	1510 ± 180	7.4 ± 3.8 (n = 5)	20%	M. Rutgers van der Loeff et al., submitted manuscript (2010)[g]
Weddell Sea	100	5.2 ± 1.4	948 ± 260	5.0 ± 1.9 (n = 9)	14%	M. Rutgers van der Loeff et al., submitted manuscript (2010)[g]
Weddell Sea	100	11.2 ± 1.6	533 ± 416	6.0 ± 5.3 (n = 3)	NR	*Rodriguez y Baena et al.* [2008][h]
Sargasso Sea	150	2.7 ± 0.9	770 ± 373	2.2 ± 1.6 (n = 63)	6%	*Buesseler et al.* [2008][i]
South China Sea	100	3.6 ± 1.2	583 ± 523	2.1 ± 2.2 (n = 36)	9%	*Cai et al.* [2008a][j]

[a] n, number of measurements of POC export; the error represents one standard deviation associated with the mean value; this also holds for POC/^{234}Th and ^{234}Th flux.
[b] NR, not reported.
[c] Results from stations with water depth >1000 m.
[d] Values from Eddy IN stations with a modeled upwelling rate of 2 m d^{-1}.
[e] Results derived during D1 deployment on the basis of a one-dimensional steady state model.
[f] Average of start and end at the Southern Ocean Iron Experiment (SOFeX) OUT station.
[g] ThE ratios were calculated using the average primary production between 50°S and 72°S from Antarctic Environment and Southern Ocean Process Study (AESOPS) 170°W cruises [*Buesseler et al.*, 2003].
[h] Steady state model results under bloom conditions.
[i] Average of the four Eddy cruises, E1–E4.
[j] Recalculated using a mean ratio of 1.8 for bottle POC/^{234}Th to pump POC/^{234}Th on >53 μm size class reported by W. Chen et al. (Spatial and seasonal variations of particle export in the northern South China Sea based on ^{234}Th:^{238}U disequilibrium, manuscript in preparation, 2010).

^{234}Th flux and POC/^{234}Th ratio on suspended particles collected on a 0.45 μm membrane filter, these investigators derived a POC export flux of 1.0 mmol m^{-2} d^{-1} at the depth horizon of 100 m. More recently, two separate studies on POC export using ^{234}Th/^{238}U were conducted by another group in the Canadian Basin of the central Arctic Ocean [*Baskaran et al.*, 2003; *Trimble and Baskaran*, 2005]. POC export fluxes were quantified to be 7.4 mmol m^{-2} d^{-1} and between 2.5 and 2.7 mmol m^{-2} d^{-1} respectively. Overall, our POC export fluxes are about one order of magnitude lower than these historical estimates (Table 2). Nevertheless, previous studies using sediment traps indicated that the POC export fluxes were in the range of 0.03–1.8 mmol m^{-2} d^{-1} in the permanently ice-covered Arctic Ocean [*Hargrave et al.*, 1994; *Fahl and Nöthig*, 2007]. By evaluating the deficit of phosphate, *Anderson et al.* [2003] have estimated an average export production of ~0.5 g C m^{-2} yr^{-1} in the central Arctic Ocean. If the growing season were 120 days in this region, then the daily export flux based on this method would be ~0.3 mmol C m^{-2} d^{-1}. On a general basis, our results are in good agreement with these independent estimates.

[32] There are several possible explanations for the discrepancy in the POC export fluxes between our study and the previous studies. First, this discrepancy might be a real reflection of the temporal-spatial variability in POC export. In this regard, it is important to note that most of the historical measurements of the ^{234}Th-based POC export were conducted in the Canadian Basin (Table 2), whereas our measurements were conducted mostly in the Eurasian Basin. Surface water in the Eurasian Basin was reported to be mainly of Atlantic origin. In contrast, the Canadian Basin is more affected by the Pacific water and the freshwater input from the Siberian rivers [e.g., *Rudels et al.*, 2000]. Compared to the Eurasian Basin, the surface water in the Canadian Basin is less saline, relatively depleted in nitrate, and much richer in silicate [*Middag et al.*, 2009]. Given the different nutrient level, it is possible that the POC export fluxes in the two Arctic basins might also be different. In the present study, several stations were occupied in the Makarov Basin, a subbasin of the Canadian Basin, and one station was occupied over the Alpha Ridge (Figure 1). However, depth profiles of total ^{234}Th revealed no significant difference in ^{234}Th deficit, and the POC export fluxes were also similar in magnitude between the Makarov Basin and the Eurasian Basin despite the contrasting nutrient regimes (Figures 7 and 9). As such, we considered that temporal-spatial variability was less likely the cause of the discrepancy in POC export between our study and the prior studies.

[33] Another possible cause of the discrepancy lies in the POC/^{234}Th ratio that was applied to POC export conversion. Overall, the POC/^{234}Th ratios in this study were in the lower range of the previous measurements (Table 2). Nevertheless,

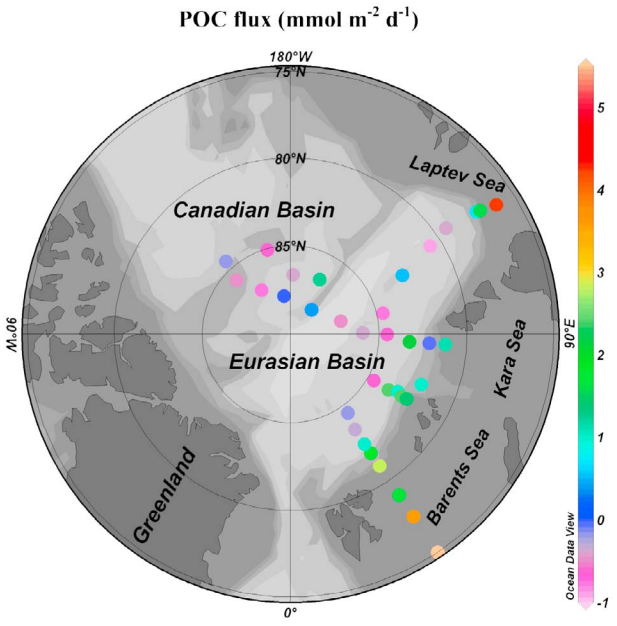

Figure 9. Geographic distribution of POC export fluxes at 100 m in the Arctic Ocean. Negative POC fluxes were likely caused by the uncertainty associated with total ^{234}Th measurements. These values were maintained in order to derive statistically accurate average of POC export fluxes in the Arctic Ocean.

it should be noted that the POC/^{234}Th measurements summarized in Table 2 were conducted on various particle size classes and via different sampling devices. Differences in POC/^{234}Th ratio between collection techniques and size variations, however, have been documented [*Buesseler et al.*, 2006]. This may in part explain the discrepancy in POC export between our study and the previous studies. It is, however, important to note that the POC/^{234}Th ratios in our study and the previous studies differed by a factor of <6. In comparison, the variability of ^{234}Th fluxes was more than one order of magnitude (Table 2). Thus, the discrepancy in POC export seemed to be mainly driven by the variability of ^{234}Th fluxes, rather than by POC/^{234}Th ratios.

[34] Finally, the discrepancy may also be caused by the methodological disparity associated with the ^{234}Th measurements. In this study, total ^{234}Th was measured using a small-volume MnO_2 coprecipitation method with addition of a ^{230}Th spike [*Buesseler et al.*, 2001; *Pike et al.*, 2005]. In comparison, most of the historical measurements of ^{234}Th/^{238}U disequilibrium listed in Table 2 relied on a MnO_2-impregnated cartridge technique. The only exception is the study by *Chen et al.* [2003], in which an $Fe(OH)_3$ coprecipitation method was invoked. Systematic offset in ^{234}Th measurements by using different methods, however, has been observed in prior studies, and the cause has been discussed [*Cai et al.*, 2006b, 2008b; *Rutgers van der Loeff et al.*, 2006; *Hung et al.*, 2008]. In an oligotrophic ocean where ^{234}Th deficit is small, a slight offset in total ^{234}Th measurements would tend to greatly bias ^{234}Th flux calculations and hence the POC flux values, as the ^{234}Th flux is determined from the difference of two large numbers [*Cai et al.*, 2006b]. Indeed, in the present study, total ^{234}Th was generally found to be in secular equilibrium with ^{238}U below 25 m in the central Arctic Ocean. In contrast, ^{234}Th deficit with respect to ^{238}U was very often found to be evident throughout the upper 200–300 m by using the MnO_2-impregnated cartridge technique. Resultantly, at a same export horizon, the average ^{234}Th flux in our study is much lower than the prior estimates (Table 2).

[35] We can also compare our results with ^{234}Th-based POC fluxes in other world oceans (Table 2). In order to minimize methodological disparity, only those studies using the small-volume MnO_2 coprecipitation method were invoked. The comparison suggests that the POC export fluxes in the central Arctic Ocean are much lower than those in other oligotrophic oceans. The low POC export resulted mainly from the low ^{234}Th fluxes in the central Arctic Ocean, which on average are about one order of magnitude lower than in other oligotrophic oceans. Notably, POC/^{234}Th ratios are similar in magnitude between the central Arctic Ocean and other oligotrophic oceans (Table 2). It should also be noted that our study was conducted in the Arctic summer, when biological productivity is typically at its highest in this area. During the long polar winter, however, biological productivity and particle export in the Arctic Ocean are generally thought to be extremely low because of the ice cover and absence of light. Indeed, strong seasonality in POC export has been recorded in the sediment traps deployed over the Lomonosov Ridge of the central Arctic Ocean, and the highest POC fluxes were seen between July and August [*Fahl and Nöthig*, 2007]. As such, our results might be regarded as the maximum of the annual POC export in the central Arctic Ocean. It is, however, important to note that the ^{234}Th/^{238}U disequilibrium approach integrates a history of POC export over 1–2 months [*Buesseler et al.*, 2006]. As such, there is a possibility that with the ^{234}Th method we might have missed the maximum export event because of a delay between plankton growth and particle export. In addition, there is a specific kind of ice algae, *Melosira arctica*, which may be of relatively large importance in the Arctic Ocean [*Zernova et al.*, 2000]. It is very patchy and grows in hairy bushes under the sea ice. Upon sea ice melt it can fall down entirely and rush down to the abyss. In fact, input of ^{234}Th-rich sea ice algae during ice melting has been observed [*Rodriguez y Baena et al.*, 2008]. Meanwhile, because of the episodic nature of such events, it is possible that we might have failed to see them with the ^{234}Th method.

[36] Low POC export in the central Arctic Ocean is most likely due to the low biological productivity in this region. Historically, the Arctic Ocean was considered to be one of the most oligotrophic oceans because of the permanent ice cover and absence of light during the long polar winter. Early measurements of biological productivity in the central Arctic Ocean generally supported this view [*English*, 1961]. Later studies, however, suggested that primary production under the permanently ice-covered Arctic may be as much as tenfold higher than the earlier measurements [*Gosselin et al.*, 1997; *Chen et al.*, 2003]. Nevertheless, the updated estimates were generally on the order of 1–10 mmol C m^{-2} d^{-1}, which is still very low compared to other oligotrophic oceans. With

low biological productivity, one may also expect to see very low POC export in the central Arctic Ocean.

[37] The ratio of ^{234}Th-derived POC export to primary production was defined as the ThE ratio [*Buesseler*, 1998]. While primary production was not determined in this study, it is still useful to compare our ^{234}Th-derived POC export to reported primary production rates in order to place our results in the context of ^{234}Th-derived POC export studies in other world oceans. *Gosselin et al.* [1997] determined an annual total primary production of 15 g C m^{-2} in the central Arctic Ocean, which included DOC release and phytoplankton production as well as ice algae production rates. Using an algae growing season of 120 days typical of this region, this estimate was converted to a daily production rate of ~10 mmol C m^{-2}. In another study, *Chen et al.* [2003] measured a primary production rate of 3.8 mmol C m^{-2} d^{-1} in the Canadian Basin, but this estimate did not include DOC release and ice algae production rates. On the basis of these results, a ThE ratio of <6% was estimated for the central Arctic Ocean. This value is comparable to the ThE ratios reported for other oligotrophic seas (see *Buesseler* [1998] and Table 2) and is also consistent with a previous conclusion, based on phosphate deficits, that extensive cycling of nutrients occurred in the upper central Arctic Ocean such that export production is at least an order of magnitude lower than total production [*Anderson et al.*, 2003]. It indicates that like other oligotrophic regimes, the central Arctic Ocean is characterized by low POC export relative to primary production, i.e., a tightly coupled food web.

5. Summary

[38] The role of the central Arctic Ocean in C sequestration is still controversial. An early view was that the central Arctic Ocean is one of the most unproductive regions in the world, due primarily to the ice cover and lack of light during the long polar winter. An implication of this view was that export fluxes of POC and associated reactive elements in the central Arctic Ocean may be lower than in other open oceans. In fact, this consideration had led some researchers to believe that total ^{234}Th was in secular equilibrium with ^{238}U under the permanent ice cap [*Bacon et al.*, 1989]. Later studies in the mid-1990s, however, had challenged this early view. *Gosselin et al.* [1997] showed that primary production under the permanently ice-covered Arctic Ocean may be as much as one order of magnitude higher than early measurements. In the meantime, ^{234}Th-based studies, although limited, generally suggested that POC export fluxes in the central Arctic Ocean were more comparable to other open oceans.

[39] In the summer of 2007, when sea ice cover in the Arctic Ocean dropped to the lowest record by far [*Comiso et al.*, 2008], we conducted a high-resolution study of POC export using ^{234}Th/^{238}U disequilibrium on board R/V *Polarstern*. Samples were processed using a small-volume MnO_2 coprecipitation method with addition of a yield tracer, which resulted in one of the most complete and theoretically accurate ^{234}Th data set ever collected. POC fluxes were determined with a steady state ^{234}Th model and pump-normalized POC/^{234}Th ratios on total suspended particles collected at 100 m. Our major findings are the very low and uniform POC export in the central Arctic Ocean and the relatively enhanced POC export over the Arctic shelves. On average, POC export fluxes over the various Arctic shelves were 2.7 ± 1.7 mmol m^{-2} d^{-1} (the Barents Sea), 0.5 ± 0.8 mmol m^{-2} d^{-1} (the Kara Sea), and 2.9 ± 1.8 mmol m^{-2} d^{-1} (the Laptev Sea), respectively. In comparison, the central Arctic Ocean was characterized by the lowest POC export flux ever reported, 0.2 ± 1.0 mmol m^{-2} d^{-1} (1 standard deviation, n = 26). This value is very low compared to prior estimates and is also much lower than the POC export fluxes reported in other oligotrophic oceans. Nonetheless, they are in good agreement with the low sediment trap-based POC export and the low export production evaluated from phosphate deficits in the permanently ice-covered Arctic Ocean [*Hargrave et al.*, 1994; *Anderson et al.*, 2003; *Fahl and Nöthig*, 2007]. A ThE ratio of <6% in the central Arctic Ocean was estimated using historical measurements of primary production. The low ThE ratio indicates that like other oligotrophic regimes, the central Arctic Ocean is characterized by low POC export relative to primary production. Our study strongly suggests that the current role of the central Arctic Ocean in C sequestration is still very limited. Meanwhile, this role may be altered because of global warming and future decline in sea ice cover. In order to understand the impact of the shrinking sea ice cover on the POC export in the central Arctic Ocean, future research should focus on time series studies, both on a seasonal scale and on a decadal scale.

[40] Finally, we have introduced a concept of minimum detection limit to POC export studies using the ^{234}Th method. We contend that the concept of a MDL is particularly important for POC export studies as most of the oligotrophic oceans are characterized with relatively small ^{234}Th deficit. The MDL of POC export is determined by two terms: the uncertainty associated with ^{234}Th flux calculation and uncertainty associated with the POC/^{234}Th ratio on sinking particles. Given total errors on the ^{234}Th/^{238}U ratio of 3%–5%, a typical sampling resolution of five depths over the upper 100 m, and a POC/^{234}Th ratio of 4.1 μmol dpm^{-1}, we have estimated a MDL of ~1.5 mmol m^{-2} d^{-1} for the Arctic coastal and open oceans. We found that most of the POC export fluxes measured in the central Arctic Ocean were below this detection threshold. Nonetheless, with the high vertical and spatial resolution we were still allowed to place a robust constraint on the average POC export in this regime. This is mainly due to the fact that the uncertainty associated with the average POC export flux decreased with increasing spatial resolution. In order to extend the use of the ^{234}Th method in low-export environments, future efforts aiming to lower the uncertainty associated with total ^{234}Th and ^{238}U measurements should be encouraged.

Appendix A

[41] Potential temperature, salinity, size-fractionated ^{234}Th, total ^{234}Th, ^{238}U and POC data in the upper Arctic Ocean. Potential temperature, salinity, total ^{234}Th and ^{238}U activities are provided in Table A1. Size-fractionated ^{234}Th and POC concentration at the export horizon are provided in Table A2.

Table A1. Potential Temperature, Salinity, Total ^{234}Th, and ^{238}U Activities in the Upper Arctic Ocean

Depth (m)	Temperature (°C)	Salinity	$^{234}Th_{Total}$ (dpm L^{-1})	Uranium-238 (dpm L^{-1})	Thorium-234/Uranium-238
			PS70-228; 75° 0.058'N, 34° 0.090'E; 176 m		
5	6.5367	35.0044	1.77 ± 0.07	2.50 ± 0.07	0.71 ± 0.03
25	3.9743	35.0303	2.15 ± 0.07	2.50 ± 0.07	0.86 ± 0.04
50	2.6515	35.0911	2.30 ± 0.08	2.50 ± 0.08	0.92 ± 0.04
75	2.1858	35.0763	2.06 ± 0.07	2.50 ± 0.08	0.82 ± 0.04
100	1.3344	35.0485	2.11 ± 0.07	2.50 ± 0.07	0.84 ± 0.04
			PS70-236; 77° 30.040'N, 33° 58.390'E; 184 m		
5	2.8965	33.9240	2.17 ± 0.07	2.42 ± 0.07	0.90 ± 0.04
25	−0.1556	34.2870	2.14 ± 0.07	2.44 ± 0.07	0.88 ± 0.04
50	−1.5581	34.5169	2.10 ± 0.07	2.46 ± 0.07	0.85 ± 0.04
75	−1.4674	34.5643	2.35 ± 0.07	2.46 ± 0.07	0.95 ± 0.04
100	0.3197	34.7330	2.20 ± 0.07	2.48 ± 0.07	0.89 ± 0.04
			PS70-237; 78° 59.790'N, 33° 58.270'E; 264 m		
5	2.7001	33.7525	1.89 ± 0.07	2.41 ± 0.07	0.79 ± 0.04
25	−1.2459	34.1839	2.20 ± 0.07	2.44 ± 0.07	0.90 ± 0.04
50	−1.5867	34.3108	2.34 ± 0.08	2.45 ± 0.07	0.96 ± 0.04
75	−1.1616	34.4639	2.25 ± 0.07	2.46 ± 0.07	0.92 ± 0.04
100	−0.9353	34.5031	2.40 ± 0.08	2.46 ± 0.07	0.97 ± 0.04
			PS70-239; 81° 00.306'N, 34° 03.055'E; 214 m		
5	−0.6508	32.0647	1.60 ± 0.06	2.29 ± 0.07	0.70 ± 0.03
25	−0.8067	33.9025	1.95 ± 0.07	2.42 ± 0.07	0.81 ± 0.04
50	−0.5589	34.3427	2.04 ± 0.07	2.45 ± 0.07	0.83 ± 0.04
75	0.1565	34.4762	1.91 ± 0.07	2.46 ± 0.07	0.78 ± 0.04
100	0.6958	34.6134	1.94 ± 0.07	2.47 ± 0.07	0.79 ± 0.04
			PS70-243; 81° 43.804'N, 33° 59.552'E; 1533 m		
5	−1.3077	32.2669	1.59 ± 0.06	2.30 ± 0.07	0.69 ± 0.03
25	−1.5667	33.9184	2.49 ± 0.08	2.42 ± 0.07	1.03 ± 0.05
50	−1.1397	34.2501	2.57 ± 0.08	2.44 ± 0.07	1.05 ± 0.05
100	1.5371	34.4959	2.69 ± 0.09	2.46 ± 0.07	1.10 ± 0.05
150	2.5595	34.7390	2.51 ± 0.08	2.48 ± 0.07	1.01 ± 0.05
200	2.7960	34.9264	2.79 ± 0.09	2.49 ± 0.07	1.12 ± 0.05
			PS70-246; 81° 52.715'N, 34° 01.369'E; 2004 m		
5	−1.4009	32.7100	1.33 ± 0.05	2.33 ± 0.07	0.57 ± 0.03
25	−1.6033	34.0301	2.22 ± 0.07	2.43 ± 0.07	0.91 ± 0.04
50	−1.2400	34.3444	2.31 ± 0.07	2.45 ± 0.07	0.94 ± 0.04
75	1.0769	34.6476	2.38 ± 0.07	2.47 ± 0.07	0.97 ± 0.04
100	2.1781	34.8357	2.51 ± 0.08	2.48 ± 0.07	1.01 ± 0.04
150	2.6419	34.9372	2.45 ± 0.08	2.49 ± 0.07	0.98 ± 0.04
200	2.7151	34.9731	2.59 ± 0.09	2.49 ± 0.07	1.04 ± 0.05
			PS70-255; 82° 30.848'N, 33 ° 55.247'E; 3115 m		
5	−1.4852	33.1812	1.78 ± 0.07	2.37 ± 0.07	0.75 ± 0.04
25	−1.6314	34.2124	2.39 ± 0.08	2.44 ± 0.07	0.98 ± 0.04
50	−1.5868	34.3034	2.27 ± 0.07	2.45 ± 0.07	0.93 ± 0.04
75	0.9227	34.6177	2.48 ± 0.08	2.47 ± 0.07	1.01 ± 0.04
100	2.1550	34.8106	2.53 ± 0.09	2.48 ± 0.07	1.02 ± 0.05
150	2.6535	34.9317	2.37 ± 0.10	2.49 ± 0.07	0.95 ± 0.05
200	2.6484	34.9618	2.36 ± 0.08	2.49 ± 0.07	0.95 ± 0.04
			PS70-257; 83 ° 29.861'N, 34 ° 02.595'E; 3970 m		
5[a]	−1.6489	33.7783	2.32 ± 0.10	2.41 ± 0.07	0.96 ± 0.05
25[a]	−1.6598	33.9105	2.51 ± 0.10	2.42 ± 0.07	1.04 ± 0.05
50[a]	−1.7964	34.1913	2.46 ± 0.10	2.44 ± 0.07	1.01 ± 0.05
75[a]	−1.7787	34.2225	2.43 ± 0.10	2.44 ± 0.07	1.00 ± 0.05
100[a]	−0.2092	34.4730	2.59 ± 0.11	2.46 ± 0.07	1.06 ± 0.05
150[a]	1.9967	34.8329	2.57 ± 0.11	2.48 ± 0.07	1.04 ± 0.05
200[a]	2.2342	34.9044	2.64 ± 0.11	2.49 ± 0.07	1.06 ± 0.05
			PS70-260; 84° 30.099'N, 36° 05.015'E; 4056 m		
5[a]	−1.6728	33.8614	2.33 ± 0.10	2.41 ± 0.07	0.97 ± 0.05
25[a]	−1.7050	34.0272	2.44 ± 0.10	2.43 ± 0.07	1.00 ± 0.05
50[a]	−1.8203	34.1835	2.53 ± 0.10	2.44 ± 0.07	1.04 ± 0.05
75[a]	−1.8336	34.2029	2.44 ± 0.10	2.44 ± 0.07	1.00 ± 0.05
100[a]	−1.7915	34.2514	2.49 ± 0.10	2.44 ± 0.07	1.02 ± 0.05
150[a]	1.2918	34.6852	2.55 ± 0.11	2.47 ± 0.07	1.03 ± 0.05
200[a]	2.0233	34.8640	2.52 ± 0.10	2.49 ± 0.07	1.01 ± 0.05
			PS70-261; 84° 38.720'N, 60° 56.020'E; 3854 m		
5	−1.5902	33.3820	2.40 ± 0.08	2.38 ± 0.07	1.01 ± 0.05
25	−1.6979	33.9838	2.52 ± 0.08	2.42 ± 0.07	1.04 ± 0.05
50	−1.8235	34.1618	2.44 ± 0.08	2.44 ± 0.07	1.00 ± 0.04
75	−1.8376	34.1843	2.49 ± 0.08	2.44 ± 0.07	1.02 ± 0.05
100	−1.1700	34.2787	2.53 ± 0.08	2.44 ± 0.07	1.03 ± 0.05
150	1.2675	34.6843	2.52 ± 0.09	2.47 ± 0.07	1.02 ± 0.05
200	2.2270	34.8750	2.41 ± 0.08	2.49 ± 0.07	0.97 ± 0.04

Table A1. (continued)

Depth (m)	Temperature (°C)	Salinity	$^{234}Th_{Total}$ (dpm L^{-1})	Uranium-238 (dpm L^{-1})	Thorium-234/Uranium-238
			PS70-264; 83° 38.502'N, 60° 25.723'E; 3494 m		
5	−1.6485	33.5551	2.06 ± 0.07	2.39 ± 0.07	0.86 ± 0.04
25	−1.6673	34.0042	2.08 ± 0.07	2.42 ± 0.07	0.86 ± 0.04
50	−1.7742	34.1617	2.33 ± 0.08	2.44 ± 0.07	0.95 ± 0.04
75	−1.6352	34.2240	2.34 ± 0.08	2.44 ± 0.07	0.96 ± 0.04
100	0.9765	34.5590	2.48 ± 0.08	2.46 ± 0.07	1.01 ± 0.05
150	2.9226	34.9294	2.36 ± 0.08	2.49 ± 0.07	0.95 ± 0.04
200	2.9022	34.9563	2.51 ± 0.08	2.49 ± 0.07	1.01 ± 0.04
			PS70-266; 83°07.643'N, 61° 48.491'E; 2993 m		
5	−1.6415	33.0568	1.80 ± 0.07	2.36 ± 0.07	0.77 ± 0.04
25	−1.4269	34.0598	2.35 ± 0.08	2.43 ± 0.07	0.97 ± 0.04
50	1.3336	34.5804	2.39 ± 0.08	2.47 ± 0.07	0.97 ± 0.04
75	2.4770	34.8337	2.37 ± 0.08	2.48 ± 0.07	0.95 ± 0.04
100	2.6614	34.8826	2.43 ± 0.08	2.49 ± 0.07	0.98 ± 0.04
150	2.7240	34.9393	2.54 ± 0.08	2.49 ± 0.07	1.02 ± 0.05
200	2.6373	34.9565	2.72 ± 0.09	2.49 ± 0.07	1.09 ± 0.05
			PS70-268; 82° 48.370'N, 60° 47.820'E; 1575 m		
5	−1.6190	32.8299	1.69 ± 0.06	2.34 ± 0.07	0.72 ± 0.04
25	−1.5034	33.8503	2.11 ± 0.07	2.41 ± 0.07	0.88 ± 0.04
50	0.1494	34.5357	2.27 ± 0.08	2.46 ± 0.07	0.92 ± 0.04
75	1.9919	34.8201	2.22 ± 0.08	2.48 ± 0.07	0.90 ± 0.04
100	2.4164	34.8840	2.32 ± 0.08	2.49 ± 0.07	0.93 ± 0.04
150	2.5815	34.9361	2.30 ± 0.08	2.49 ± 0.07	0.92 ± 0.04
200	2.4851	34.9526	2.35 ± 0.08	2.49 ± 0.07	0.94 ± 0.04
			PS70-271; 82° 30.180'N, 60° 47.710'E; 327 m		
5	−1.5187	32.8458	1.88 ± 0.07	2.34 ± 0.07	0.80 ± 0.04
25	−1.5574	33.9708	2.22 ± 0.08	2.42 ± 0.07	0.92 ± 0.04
50	0.6888	34.6341	2.47 ± 0.08	2.47 ± 0.07	1.00 ± 0.04
75	1.4891	34.7928	2.46 ± 0.08	2.48 ± 0.07	0.99 ± 0.04
100	2.0460	34.8610	2.35 ± 0.08	2.49 ± 0.07	0.94 ± 0.04
150	2.1648	34.9123	2.39 ± 0.08	2.49 ± 0.07	0.96 ± 0.04
200	2.0485	34.9335	2.29 ± 0.08	2.49 ± 0.07	0.92 ± 0.04
			PS70-276; 82° 05.091'N, 68° 57.169'E; 662 m		
5[a]	−1.6925	32.9036	1.99 ± 0.08	2.35 ± 0.07	0.85 ± 0.04
25[a]	−1.5786	33.8140	2.18 ± 0.09	2.41 ± 0.07	0.90 ± 0.05
50[a]	−1.6287	34.3342	2.33 ± 0.09	2.45 ± 0.07	0.95 ± 0.05
75[a]	−0.4666	34.5140	2.41 ± 0.10	2.46 ± 0.07	0.98 ± 0.05
100[a]	1.8002	34.7945	2.43 ± 0.10	2.48 ± 0.07	0.98 ± 0.05
150[a]	2.4742	34.9029	2.51 ± 0.10	2.49 ± 0.07	1.01 ± 0.05
200[a]	2.4033	34.9207	2.54 ± 0.10	2.49 ± 0.07	1.02 ± 0.05
			PS70-279; 81° 13.808'N, 86° 10.759'E; 316 m		
5	−1.4971	32.6448	2.05 ± 0.07	2.33 ± 0.07	0.88 ± 0.04
25	−1.6348	33.9594	2.32 ± 0.08	2.42 ± 0.07	0.96 ± 0.04
50	−0.7807	34.5311	2.48 ± 0.08	2.46 ± 0.07	1.01 ± 0.04
75	0.8474	34.7568	2.27 ± 0.08	2.48 ± 0.07	0.91 ± 0.04
100	1.2217	34.8463	2.40 ± 0.08	2.48 ± 0.07	0.97 ± 0.04
150	0.8876	34.8802	2.45 ± 0.08	2.49 ± 0.07	0.98 ± 0.04
200	−0.6718	34.8056	2.56 ± 0.08	2.48 ± 0.07	1.03 ± 0.05
			PS70-285; 82° 08.500'N, 86° 19.850'E; 723 m		
5	−1.6253	32.5168	2.14 ± 0.07	2.32 ± 0.07	0.92 ± 0.04
25	−1.5823	33.4152	2.35 ± 0.08	2.38 ± 0.07	0.99 ± 0.05
50	−0.9526	34.3039	2.53 ± 0.08	2.45 ± 0.07	1.03 ± 0.05
75	−1.7537	34.4288	2.50 ± 0.08	2.45 ± 0.07	1.02 ± 0.05
100	−1.4392	34.4794	2.48 ± 0.08	2.46 ± 0.07	1.01 ± 0.05
150	0.1621	34.6825	2.42 ± 0.08	2.47 ± 0.07	0.98 ± 0.04
200	1.1092	34.8151	2.49 ± 0.08	2.48 ± 0.07	1.00 ± 0.05
			PS70-295; 83° 16.330'N, 86° 17.030'E; 3357 m		
5	−1.6482	33.3319	2.23 ± 0.07	2.38 ± 0.07	0.94 ± 0.04
25	−1.6430	33.9985	2.20 ± 0.07	2.42 ± 0.07	0.91 ± 0.04
50	−1.7567	34.1796	2.24 ± 0.07	2.44 ± 0.07	0.92 ± 0.04
75	−1.7688	34.2254	2.35 ± 0.08	2.44 ± 0.07	0.96 ± 0.04
100	−1.3615	34.3235	2.26 ± 0.07	2.45 ± 0.07	0.93 ± 0.04
150	2.7044	34.8716	2.41 ± 0.08	2.49 ± 0.07	0.97 ± 0.04
200	2.8560	34.9393	2.43 ± 0.08	2.49 ± 0.07	0.97 ± 0.04
			PS70-301; 84° 33.645'N, 89° 48.780'E; 3751 m		
5[a]	−1.6458	33.3433	1.95 ± 0.08	2.38 ± 0.07	0.82 ± 0.04
25[a]	−1.6848	33.6530	2.55 ± 0.10	2.40 ± 0.07	1.06 ± 0.05
50[a]	−1.8103	34.0067	2.60 ± 0.10	2.42 ± 0.07	1.07 ± 0.05
75[a]	−1.6488	34.1233	2.44 ± 0.10	2.43 ± 0.07	1.00 ± 0.05
100[a]	−0.8639	34.3054	2.42 ± 0.10	2.45 ± 0.07	0.99 ± 0.05
150[a]	0.8363	34.6427	2.59 ± 0.10	2.47 ± 0.07	1.05 ± 0.05
200[a]	1.8087	34.8386	2.56 ± 0.10	2.48 ± 0.07	1.03 ± 0.05

Table A1. (continued)

Depth (m)	Temperature (°C)	Salinity	$^{234}Th_{Total}$ (dpm L^{-1})	Uranium-238 (dpm L^{-1})	Thorium-234/Uranium-238
PS-306; 85° 55.370'N, 91° 07.330'E; 4019 m					
5[a]	−1.6802	32.3133	2.08 ± 0.09	2.30 ± 0.07	0.90 ± 0.05
25[a]	−1.6874	33.4580	2.61 ± 0.10	2.39 ± 0.07	1.09 ± 0.06
50[a]	−1.8037	33.7654	2.53 ± 0.10	2.41 ± 0.07	1.05 ± 0.05
75[a]	−1.7341	33.9052	2.54 ± 0.10	2.42 ± 0.07	1.05 ± 0.05
100[a]	−1.2921	34.2094	2.51 ± 0.10	2.44 ± 0.07	1.03 ± 0.05
150[a]	0.0443	34.5286	2.54 ± 0.10	2.46 ± 0.07	1.03 ± 0.05
200[a]	1.0343	34.7767	2.58 ± 0.10	2.48 ± 0.07	1.04 ± 0.05
PS70-309; 87° 02.554'N, 104° 55.831'E; 4459 m					
5	−1.6881	31.7575	2.07 ± 0.07	2.26 ± 0.07	0.91 ± 0.04
25	−1.6855	32.6497	2.41 ± 0.08	2.33 ± 0.07	1.03 ± 0.05
50	−1.7597	33.1346	2.46 ± 0.08	2.36 ± 0.07	1.04 ± 0.05
75	−1.6332	33.8730	2.47 ± 0.08	2.42 ± 0.07	1.02 ± 0.05
100	−1.2990	34.2110	2.52 ± 0.08	2.44 ± 0.07	1.03 ± 0.05
150	−0.0218	34.5275	2.52 ± 0.08	2.46 ± 0.07	1.02 ± 0.05
200	1.0280	34.7906	2.25 ± 0.08	2.48 ± 0.07	0.91 ± 0.04
PS70-316; 88° 10.620'N, 139° 36.980'E; 1298 m					
5	−1.6774	31.1637	1.99 ± 0.07	2.22 ± 0.07	0.90 ± 0.04
25	−1.6410	31.8820	2.26 ± 0.08	2.27 ± 0.07	0.99 ± 0.05
50	−1.7180	32.5177	2.35 ± 0.08	2.32 ± 0.07	1.01 ± 0.05
75	−1.6061	33.8421	2.37 ± 0.08	2.41 ± 0.07	0.98 ± 0.04
100	−1.3128	34.1801	2.47 ± 0.08	2.44 ± 0.07	1.01 ± 0.05
150	−0.0249	34.5042	2.41 ± 0.08	2.46 ± 0.07	0.98 ± 0.04
200	1.0551	34.7825	2.57 ± 0.08	2.48 ± 0.07	1.04 ± 0.05
PS70-328; 87° 49.295'N, 170° 18.573'W; 3993 m					
5[a]	−1.5391	28.9468	1.97 ± 0.09	2.06 ± 0.06	0.95 ± 0.05
25[a]	−1.5318	30.2788	2.23 ± 0.09	2.16 ± 0.06	1.03 ± 0.05
50[a]	−1.6543	31.0747	2.21 ± 0.09	2.22 ± 0.07	1.00 ± 0.05
75[a]	−1.6067	33.1995	2.39 ± 0.10	2.37 ± 0.07	1.01 ± 0.05
100[a]	−1.5256	33.9607	2.35 ± 0.10	2.42 ± 0.07	0.97 ± 0.05
150[a]	−0.5404	34.3968	2.47 ± 0.10	2.45 ± 0.07	1.01 ± 0.05
200[a]	0.2931	34.6273	2.59 ± 0.10	2.47 ± 0.07	1.05 ± 0.05
PS70-333; 88° 10.620'N, 139° 36.980'W; 3300 m					
5[a]	−1.5501	28.7277	2.11 ± 0.08	2.05 ± 0.06	1.03 ± 0.05
25[a]	−1.5385	28.8438	2.03 ± 0.08	2.06 ± 0.06	0.99 ± 0.05
50[a]	−1.5681	30.1091	2.23 ± 0.09	2.15 ± 0.06	1.04 ± 0.05
75[a]	−1.6091	33.1656	2.44 ± 0.09	2.36 ± 0.07	1.03 ± 0.05
100[a]	−1.5420	33.9081	2.44 ± 0.09	2.42 ± 0.07	1.01 ± 0.05
150[a]	−0.8022	34.3575	2.46 ± 0.10	2.45 ± 0.07	1.00 ± 0.05
200[a]	0.0416	34.5865	2.47 ± 0.10	2.47 ± 0.07	1.00 ± 0.05
PS70-338; 85° 42.084'N, 135° 01.570'W; 1529 m					
5	−1.5354	28.5850	2.06 ± 0.07	2.04 ± 0.06	1.01 ± 0.05
25	−1.3920	29.6248	2.19 ± 0.07	2.11 ± 0.06	1.04 ± 0.05
50	−1.5867	30.2997	2.21 ± 0.07	2.16 ± 0.06	1.02 ± 0.05
75	−1.5333	31.9056	2.32 ± 0.08	2.27 ± 0.07	1.02 ± 0.05
100	−1.5002	33.2714	2.40 ± 0.08	2.37 ± 0.07	1.01 ± 0.05
150	−0.9504	34.2266	2.32 ± 0.07	2.44 ± 0.07	0.95 ± 0.04
200	−0.1331	34.5176	2.43 ± 0.07	2.46 ± 0.07	0.99 ± 0.04
PS70-342; 84° 29.936'N, 138° 24.019'W; 2220 m					
5	−1.4701	29.2901	2.02 ± 0.06	2.09 ± 0.06	0.97 ± 0.04
25	−1.4356	30.2968	2.24 ± 0.07	2.16 ± 0.06	1.04 ± 0.04
50	−1.5906	30.5100	2.14 ± 0.07	2.18 ± 0.07	0.98 ± 0.04
75	−1.5063	31.4757	2.26 ± 0.07	2.24 ± 0.07	1.01 ± 0.04
100	−1.3833	32.4991	2.40 ± 0.07	2.32 ± 0.07	1.04 ± 0.04
150	−1.1995	34.0809	2.28 ± 0.07	2.43 ± 0.07	0.94 ± 0.04
200	−0.4223	34.4127	2.38 ± 0.08	2.45 ± 0.07	0.97 ± 0.04
PS70-349; 85° 4.275'N, 164° 32.311'W; 1968 m					
5[a]	−1.3987	26.9659	1.90 ± 0.08	1.92 ± 0.06	0.99 ± 0.05
25[a]	−1.4834	29.0032	2.10 ± 0.09	2.07 ± 0.06	1.01 ± 0.05
50[a]	−1.5426	31.1274	2.35 ± 0.10	2.22 ± 0.07	1.06 ± 0.05
75[a]	−1.5531	32.8902	2.43 ± 0.10	2.35 ± 0.07	1.04 ± 0.05
100[a]	−1.5447	33.8690	2.36 ± 0.10	2.41 ± 0.07	0.98 ± 0.05
150[a]	−0.6989	34.3371	2.43 ± 0.09	2.45 ± 0.07	0.99 ± 0.04
200[a]	0.1574	34.5988	2.55 ± 0.10	2.47 ± 0.07	1.03 ± 0.05
PS70-352; 86° 38.688'N, 177° 33.764'E; 3988 m					
5[a]	−1.5884	29.5240	2.01 ± 0.09	2.11 ± 0.06	0.95 ± 0.05
25[a]	−1.6291	30.3274	2.13 ± 0.09	2.16 ± 0.06	0.98 ± 0.05
50[a]	−1.6601	31.7611	2.43 ± 0.10	2.26 ± 0.07	1.07 ± 0.05
75[a]	−1.5551	33.4769	2.42 ± 0.10	2.39 ± 0.07	1.01 ± 0.05
100[a]	−1.4733	34.0337	2.45 ± 0.10	2.43 ± 0.07	1.01 ± 0.05
150[a]	−0.3144	34.4597	2.45 ± 0.09	2.46 ± 0.07	1.00 ± 0.05
200[a]	0.4435	34.6833	2.51 ± 0.10	2.47 ± 0.07	1.01 ± 0.05

Table A1. (continued)

Depth (m)	Temperature (°C)	Salinity	$^{234}Th_{Total}$ (dpm L^{-1})	Uranium-238 (dpm L^{-1})	Thorium-234/Uranium-238
			PS70-358; 86° 30.228'N, 151° 58.641'E; 1424 m		
5	−1.6622	30.8922	1.90 ± 0.07	2.20 ± 0.07	0.86 ± 0.04
25	−1.6142	31.1867	2.05 ± 0.07	2.22 ± 0.07	0.92 ± 0.04
50	−1.7010	32.9265	2.44 ± 0.08	2.35 ± 0.07	1.04 ± 0.05
75	−1.6129	33.810	2.43 ± 0.08	2.41 ± 0.07	1.01 ± 0.04
100	−1.3694	34.1366	2.40 ± 0.08	2.43 ± 0.07	0.99 ± 0.04
150	−0.2326	34.4832	2.40 ± 0.08	2.46 ± 0.07	0.97 ± 0.04
200	0.6828	34.7309	2.57 ± 0.08	2.48 ± 0.07	1.04 ± 0.05
			PS70-371; 84° 39.200'N, 102° 44.180'E; 4271 m		
5[a]	−1.6896	33.1565	2.42 ± 0.10	2.36 ± 0.07	1.02 ± 0.05
25[a]	−1.7632	33.4216	2.40 ± 0.10	2.38 ± 0.07	1.01 ± 0.05
50[a]	−1.8032	33.7251	2.44 ± 0.10	2.40 ± 0.07	1.01 ± 0.05
75[a]	−1.6781	33.9225	2.59 ± 0.10	2.42 ± 0.07	1.07 ± 0.05
100[a]	−1.1645	34.2593	2.46 ± 0.10	2.44 ± 0.07	1.01 ± 0.05
150[a]	0.1612	34.5820	2.41 ± 0.09	2.47 ± 0.07	0.98 ± 0.05
200[a]	1.0328	34.8479	2.55 ± 0.10	2.48 ± 0.07	1.03 ± 0.05
			PS70-379; 82° 11.699'N, 119° 33.653'E; 4418 m		
5	−1.6627	31.1065	1.93 ± 0.06	2.22 ± 0.07	0.87 ± 0.04
25	−1.6806	32.6984	2.39 ± 0.07	2.33 ± 0.07	1.02 ± 0.04
50	−1.7290	33.4840	2.43 ± 0.08	2.39 ± 0.07	1.02 ± 0.04
75	−1.5917	34.0557	2.41 ± 0.07	2.43 ± 0.07	0.99 ± 0.04
100	−1.0215	34.2794	2.35 ± 0.07	2.44 ± 0.07	0.96 ± 0.04
150	0.5035	34.6333	2.45 ± 0.07	2.47 ± 0.07	0.99 ± 0.04
200	1.1597	34.8267	2.58 ± 0.07	2.48 ± 0.07	1.04 ± 0.04
			PS70-383; 80° 39.570'N, 122° 13.411'E; 3890 m		
5[a]	−1.5029	31.5031	2.09 ± 0.09	2.25 ± 0.07	0.93 ± 0.05
25[a]	−1.6713	32.9505	2.40 ± 0.10	2.35 ± 0.07	1.02 ± 0.05
50[a]	−1.7887	33.7486	2.53 ± 0.10	2.41 ± 0.07	1.05 ± 0.05
75[a]	−1.6732	34.0791	2.49 ± 0.10	2.43 ± 0.07	1.03 ± 0.05
100[a]	−0.8937	34.3122	2.49 ± 0.10	2.45 ± 0.07	1.02 ± 0.05
150[a]	0.8382	34.6677	2.49 ± 0.10	2.47 ± 0.07	1.01 ± 0.05
200[a]	1.2856	34.8357	2.53 ± 0.10	2.48 ± 0.07	1.02 ± 0.05
			PS70-385; 79° 20.778'N, 124° 20.777'E; 3524 m		
5[a]	−0.9683	31.2057	1.93 ± 0.08	2.22 ± 0.07	0.87 ± 0.05
25[a]	−1.6795	33.8141	2.48 ± 0.10	2.41 ± 0.07	1.03 ± 0.05
50[a]	−1.7933	33.9876	2.59 ± 0.11	2.42 ± 0.07	1.07 ± 0.05
75[a]	−1.4439	34.1913	2.47 ± 0.10	2.44 ± 0.07	1.01 ± 0.05
100[a]	−0.5946	34.3882	2.45 ± 0.10	2.45 ± 0.07	1.00 ± 0.05
150[a]	1.7034	34.7925	2.64 ± 0.10	2.48 ± 0.07	1.06 ± 0.05
200[a]	2.2347	34.9106	2.51 ± 0.10	2.49 ± 0.07	1.01 ± 0.05
			PS70-400; 77° 22.177'N, 123° 24.896'E; 1029 m		
5	−1.5873	32.1473	2.01 ± 0.07	2.29 ± 0.07	0.88 ± 0.04
25	−1.3419	33.8010	2.23 ± 0.08	2.41 ± 0.07	0.93 ± 0.04
50	−1.3893	34.2371	2.41 ± 0.08	2.44 ± 0.07	0.99 ± 0.04
75	−1.4506	34.3588	2.24 ± 0.07	2.45 ± 0.07	0.91 ± 0.04
100	−1.5505	34.4061	2.39 ± 0.08	2.45 ± 0.07	0.97 ± 0.04
150	0.4395	34.6365	2.26 ± 0.07	2.47 ± 0.07	0.92 ± 0.04
200	1.1551	34.7875	2.45 ± 0.07	2.48 ± 0.07	0.99 ± 0.04
			PS70-403; 77° 08.995'N, 123° 07.458'E; 114 m		
5	−1.6188	30.7335	1.86 ± 0.06	2.19 ± 0.07	0.85 ± 0.04
25	−1.1319	33.7607	2.04 ± 0.06	2.41 ± 0.07	0.85 ± 0.04
50	−1.2236	34.0933	1.90 ± 0.06	2.43 ± 0.07	0.78 ± 0.04
75	−1.2863	34.2418	2.05 ± 0.07	2.44 ± 0.07	0.84 ± 0.04
100	−1.3869	34.3420	2.02 ± 0.07	2.45 ± 0.07	0.83 ± 0.04
			PS70-407; 76° 10.876'N, 122°08.448'E; 72 m		
5	−0.4385	29.5306	1.59 ± 0.06	2.11 ± 0.06	0.76 ± 0.04
25	−1.5343	33.3614	1.82 ± 0.06	2.38 ± 0.07	0.77 ± 0.03
50	−1.6402	33.7589	1.45 ± 0.05	2.41 ± 0.07	0.60 ± 0.03

[a]Samples to which the average recovery of 94.8% ± 2.4% was applied.

Table A2. Size-Fractionated ^{234}Th and POC Concentration at the Export Horizon in the Arctic Ocean

	^{234}Th (dpm L^{-1})				POC (μmol L^{-1})			
Station/100 m	Bottle	1–53 μm[a]	53–100 μm	>100 μm	Bottle	1–53 μm[a]	53–100μm	>100 μm
PS70-239	0.75 ± 0.02	*0.045 ± 0.002*	0.022 ± 0.001	0.064 ± 0.001	1.9	*0.05*	0.35	0.72
PS70-255	0.27 ± 0.02	*0.032 ± 0.003*	0.003 ± 0.0002	0.028 ± 0.001	1.0	*0.08*	0.023	0.060
PS70-260	0.40 ± 0.02	*0.019 ± 0.002*	0.001 ± 0.001	0.003 ± 0.0003	1.7	*0.07*	0.007	0.032
PS70-266	0.36 ± 0.02	0.23 ± 0.01	0.004 ± 0.0003	0.015 ± 0.0005	1.2	0.38	0.014	0.035
PS70-276	0.33 ± 0.02	0.20 ± 0.01	0.007 ± 0.0003	0.020 ± 0.0007	1.0	0.44	0.021	0.050
PS70-279	0.25 ± 0.01	0.16 ± 0.01	0.007 ± 0.0003	0.005 ± 0.0003	0.8	0.34	0.014	0.017
PS70-301	0.14 ± 0.01	0.06 ± 0.003	0.001 ± 0.0002	0.001 ± 0.0002	1.4	0.23	0.006	0.015
PS70-309	0.21 ± 0.01	0.08 ± 0.004	0.002 ± 0.0002	0.003 ± 0.0002	1.1	0.19	0.007	0.015
PS70-328	0.23 ± 0.01	0.12 ± 0.01	0.003 ± 0.0003	0.003 ± 0.0002	1.9	0.56	0.012	0.017
PS70-338	0.24 ± 0.01	0.08 ± 0.01	0.002 ± 0.0002	0.002 ± 0.0002	1.0	0.17	0.008	0.009
PS70-358	0.18 ± 0.01	0.14 ± 0.01	0.002 ± 0.0003	0.009 ± 0.0004	1.7	0.48	0.016	0.033
PS70-385	0.22 ± 0.01	0.11 ± 0.01	0.003 ± 0.0003	0.005 ± 0.0003	1.4	0.34	0.010	0.015
PS70-400	0.60 ± 0.02	0.41 ± 0.01	0.004 ± 0.0003	0.011 ± 0.0005	1.2	0.50	0.010	0.017
PS70-407	1.27 ± 0.03	0.45 ± 0.01	0.070 ± 0.0002	0.034 ± 0.0001	7.5	1.9	0.44	0.20

[a]Italic numbers represent inaccurate data as the 142 mm 1.0 μm filters were found to be torn during in situ filtration. These data are not discussed in the text. Nevertheless, we assume that the POC/^{234}Th ratios were not affected by the torn filters.

[42] **Acknowledgments.** We wish to thank the chief scientist of ARK-XXII/2 expedition for organizing this cruise. We wish to thank the captain and crew of R/V Polarstern for their assistance in sample collection during the cruise. Thanks are also due to the GEOTRACES team for joint sampling and data exchange, and to Lilith Kuckero for performing chlorophyll measurements. Constructive comments by three anonymous reviewers helped to significantly improve this manuscript. Financial support from the Alexander von Humboldt Foundation to P.C. during a sabbatical leave is gratefully acknowledged. This work was supported by the National Basic Research Program ("973" Program) of China through grant 2009CB421203 and by the International Bureau of the Federal Ministry of Education and Research of Germany through grant IB-CHN 06/018.

References

Anderson, L. G., G. Björk, O. Holby, E. P. Jones, G. Kattner, K. P. Koltermann, B. Liljeblad, R. Lindegren, B. Rudels, and J. H. Swift (1994), Water masses and circulation in the Eurasian Basin: Results from the *Oden* 91 expedition, *J. Geophys. Res.*, *99*, 3273–3283.

Anderson, L. G., E. P. Jones, and J. H. Swift (2003), Export production in the central Arctic Ocean evaluated from phosphate deficits, *J. Geophys. Res.*, *108*(C6), 3199, doi:10.1029/2001JC001057.

Arrigo, K. R., G. V. Dijkin, and S. Pabi (2008), Impact of a shrinking Arctic ice cover on marine primary production, *Geophys. Res. Lett.*, *35*, L19603, doi:10.1029/2008GL035028.

Bacon, M. P., C.-A. Huh, and R. M. Moore (1989), Vertical profiles of some natural radionuclides over the Alpha Ridge, Arctic Ocean, *Earth Planet. Sci. Lett.*, *95*, 15–22.

Baskaran, M., P. M. Swarzenski, and D. Porcelli (2003), Role of colloidal material in the removal of ^{234}Th in the Canada basin of the Arctic Ocean, *Deep Sea Res., Part I*, *50*, 1353–1373.

Bates, N. R., S. B. Moran, D. A. Hansell, and J. T. Mathis (2006), An increasing CO_2 sink in the Arctic Ocean due to sea-ice loss, *Geophys. Res. Lett.*, *33*, L23609, doi:10.1029/2006GL027028.

Benitez-Nelson, C. R., K. O. Buesseler, and G. Crossin (2000), Upper ocean carbon export, horizontal transport, and vertical eddy diffusivity in the southwestern Gulf of Maine, *Cont. Shelf Res.*, *20*, 707–736.

Benitez-Nelson, C. R., K. O. Buesseler, D. Karl, and J. Andrews (2001), A time-series study of particulate matter export in the North Pacific Subtropical Gyre based upon ^{234}Th:^{238}U disequilibrium, *Deep Sea Res., Part I*, *48*, 2595–2611.

Buesseler, K. O. (1998), The decoupling of production and particulate export in the surface ocean, *Global Biogeochem. Cycles*, *12*, 297–310.

Buesseler, K. O., M. P. Bacon, J. K. Cochran, and H. D. Livingston (1992), Carbon and nitrogen export during the JGOFS North Atlantic Bloom Experiment estimated from ^{234}Th:^{238}U disequilibria, *Deep Sea Res., Part A*, *39*, 1115–1137.

Buesseler, K. O., J. E. Andrews, M. C. Hartman, R. Belastock, and F. Chai (1995), Regional estimates of the export flux of particulate organic carbon derived from thorium-234 during the JGOFS EqPac program, *Deep Sea Res., Part II*, *42*, 777–804.

Buesseler, K. O., L. Ball, J. E. Andrews, C. R. Benitez-Nelson, R. Belastock, F. Chai, and Y. Chao (1998), Upper ocean export of particulate organic carbon in the Arabian Sea derived from thorium-234, *Deep Sea Res., Part II*, *45*, 2461–2487.

Buesseler, K. O., C. R. Benitez-Nelson, M. M. Rutgers van der Loeff, J. E. Andrews, L. Ball, G. Crossin, and M. A. Charette (2001), An intercomparison of small- and large-volume techniques for thorium-234 in seawater, *Mar. Chem.*, *74*, 15–28.

Buesseler, K. O., R. T. Barber, M. L. Dickson, M. R. Hiscock, J. K. Moore, and R. Sambrotto (2003), The effect of marginal ice-edge dynamics on production and export in the Southern Ocean along 170°W, *Deep Sea Res., Part II*, *50*, 579–603.

Buesseler, K. O., J. E. Andrews, S. M. Pike, and M. A. Charette (2005), Particle export during the Southern Ocean Iron Experiment (SOFeX), *Limnol. Oceanogr.*, *50*(1), 311–327.

Buesseler, K. O., et al. (2006), An assessment of particulate organic carbon to thorium-234 ratios in the ocean and their impact on the application of ^{234}Th as a POC flux proxy, *Mar. Chem.*, *100*, 213–233.

Buesseler, K. O., C. Lamborg, P. Cai, E. Escoube, R. Johnson, S. Pike, P. Masque, D. McGillicuddy, and E. Verdeny (2008), Particle fluxes associated with mesoscale eddies in the Sargasso Sea, *Deep Sea Res., Part II*, *55*, 1426–1444.

Buesseler, K. O., S. Pike, K. Maiti, C. Lamborg, D. A. Siegel, and T. W. Trull (2009), Thorium-234 as a tracer of spatial, temporal and vertical variability in particle flux in the North Pacific, *Deep Sea Res., Part I*, *56*, 1143–1167.

Cai, P., M. Dai, D. Lv, and W. Chen (2006a), An improvement in the small-volume technique for determining thorium-234 in seawater, *Mar. Chem.*, *100*, 282–288.

Cai, P., M. Dai, D. Lv, and W. Chen (2006b), How accurate are ^{234}Th measurements in seawater based on the MnO_2-impregnated cartridge technique?, *Geochem. Geophys. Geosyst.*, *7*, Q03020, doi:10.1029/2005GC001104.

Cai, P., M. Dai, W. Chen, T. Tang, and K. Zhou (2006c), On the importance of the decay of ^{234}Th in determining size-fractionated C/^{234}Th ratio on marine particles, *Geophys. Res. Lett.*, *33*, L23602, doi:10.1029/2006GL027792.

Cai, P., W. Chen, M. Dai, Z. Wan, D. Wang, Q. Li, T. Tang, and D. Lv (2008a), A high-resolution study of particle export in the southern South China Sea based on ^{234}Th:^{238}U disequilibrium, *J. Geophys. Res.*, *113*, C04019, doi:10.1029/2007JC004268.

Cai, P., M. Dai, D. Lv, W. Chen (2008b), Reply to comment by Chin-Chang Hung et al. on "How accurate are ^{234}Th measurements in seawater based on the MnO_2-impregnated cartridge technique?", *Geochem. Geophys. Geosyst.*, *9*, Q02010, doi:10.1029/2007GC001837.

Charette, M. A., S. B. Moran, S. M. Pike, and J. N. Smith (2001), Investigating the carbon cycle in the Gulf of Maine using the natural tracer thorium-234, *J. Geophys. Res.*, *106*(C6), 11,553–11,579.

Chen, M., Y. Huang, P. Cai, and L. Guo (2003), Particulate organic carbon export fluxes in the Canada Basin and Bering Sea as derived from ^{234}Th/^{238}U disequilibria, *Arctic*, *56*, 32–44.

Comiso, J. C., C. L. Parkinson, R. Gersten, and L. Stock (2008), Accelerated decline in the Arctic sea ice cover, *Geophys. Res. Lett.*, *35*, L01703, doi:10.1029/2007GL031972.

Coppola, L., M. Roy-Barman, P. Wassmann, S. Mulsow, and C. Jeandel (2002), Calibration of sediment trap and particulate organic carbon export using ^{234}Th in the Barents Sea, *Mar. Chem.*, *80*, 11–26.

English, T. S. (1961), Some biological oceanographic observations in the central North Sea, Drift Station Alpha, 1957–1958, *Rep. 13*, pp. 8–80, Arctic Inst. of North Am., Calgary, Alta., Canada.

Fahl, K., and E.-M. Nöthig (2007), Lithogenic and biogenic particle fluxes on the Lomonosov Ridge (central Arctic Ocean) and their relevance for sediment accumulation: Vertical vs. lateral transport, *Deep Sea Res., Part I*, *54*, 1256–1272.

Gosselin, M., M. Levasseur, P. A. Wheeler, B. C. Booth, and R. A. Horner (1997), New measurements of phytoplankton and ice algal production in the Arctic Ocean, *Deep Sea Res., Part II*, *44*, 1623–1644.

Hargrave, B. T., B. V. Bodungen, P. Stoffyn-Egli, and P. J. Mudie (1994), Seasonal variability in particle sedimentation under permanent ice cover in the Arctic Ocean, *Cont. Shelf Res.*, *14*, 279–293.

Huang, Y., D. Jiang, M. Xu, M. Chen, and Y. Qiu (1997), A study on horizontal eddy diffusion in the surface water of the northeastern South China Sea based on ^{228}Ra tracer, *Trop. Oceanol.*, *16*, 67–74.

Hung, C.-C., S. B. Moran, J. K. Cochran, L. Guo, and P. H. Santschi (2008), Comment on "How accurate are ^{234}Th measurements in seawater based on the MnO_2-impregnated cartridge technique?" by Pinghe Cai et al., *Geochem. Geophys. Geosyst.*, *9*, Q02009, doi:10.1029/2007GC001770.

Knap, A., A. Michaels, A. Close, H. Ducklow, and A. Dickson (1994), Protocols for the Joint Global Ocean Flux Study (JGOFS) core measurements, *Manuals Guides No. 29*, Intergov. Oceanogr. Comm. (UNESCO), Paris.

Knap, A., A. Michaels, A. Close, H. Ducklow, and A. Dickson (1996), Protocols for the Joint Global Ocean Flux Study (JGOFS) core measurements, *Rep. 19*, pp. vi-170, Joint Global Ocean Flux Study, Washington, D. C.

Lalande, C., K. Lepore, L. W. Cooper, J. M. Grebmeier, and S. B. Moran (2007), Export fluxes of particulate organic carbon in the Chukchi Sea: A comparative study using ^{234}Th/^{238}U disequilibria and drifting sediment traps, *Mar. Chem.*, *103*, 185–196.

Lalande, C., S. B. Moran, P. Wassmann, J. M. Grebmeier, and L. W. Cooper (2008), ^{234}Th-derived particulate organic carbon fluxes in the northern Barents Sea with comparison to drifting sediment trap fluxes, *J. Mar. Syst.*, *73*, 103–113.

Lepore, K., S. B. Moran, J. M. Grebmeier, L. W. Cooper, C. Lalande, W. Maslowski, N. R. Bates, D. A. Hansell, J. Mathis, and R. P. Kelly (2007), Seasonal and interannual changes in POC export and deposition in the Chukchi Sea, *J. Geophys. Res.*, *112*, C10024, doi:10.1029/2006JC003555.

Liu, Z., G. Stewart, J. K. Cochran, C. Lee, R. A. Armstrong, D. J. Hirschberg, B. Gasser, and J.-C. Miquel (2005), Why do POC concentrations measured using Niskin bottle collections sometimes differ from those using in-situ pumps?, *Deep Sea Res., Part I*, *52*, 1324–1344.

Liu, Z., J. K. Cochran, C. Lee, B. Gasser, J. C. Miquel, and S. G. Wakeham (2009), Further investigations on why POC concentrations differ in samples collected by Niskin bottle and *in situ* pump, *Deep Sea Res., Part II*, *56*, doi:10.1016/j/dsr2.2008.12.019.

Maiti, K., C. R. Benitez-Nelson, Y. Rii, and R. Bidigare (2008), The influence of a mature cyclonic eddy on particle export in the lee of Hawaii, *Deep Sea Res., Part II*, *55*, 1445–1460.

Middag, R., H. J. W. de Baar, P. Laan, and K. Bakker (2009), Dissolved aluminium and the silicon cycle in the Arctic Ocean, *Mar. Chem.*, *115*, 176–195.

Moran, S. B., and J. N. Smith (2000), ^{234}Th as a tracer of scavenging and particle export in the Beaufort Sea, *Cont. Shelf Res.*, *20*, 153–167.

Moran, S. B., K. M. Ellis, and J. N. Smith (1997), ^{234}Th/^{238}U disequilibrium in the central Arctic Ocean: Implications for particulate organic carbon export, *Deep Sea Res., Part II*, *44*, 1593–1606.

Moran, S. B., et al. (2005), Seasonal changes in POC export flux in the Chukchi Sea and implications for water column-benthic coupling in Arctic shelves, *Deep Sea Res. II*, *52*, 3427–3451.

Overland, J. E., and M. Wang (2007), Future regional Arctic sea ice declines, *Geophys. Res. Lett.*, *34*, L17705, doi:10.1029/2007GL030308.

Pates, J. M., and G. K. P. Muir (2007), U-salinity relationships in the Mediterranean: Implications for ^{234}Th:^{238}U particle flux studies, *Mar. Chem.*, *106*, 530–545.

Pike, S. M., K. O. Buesseler, J. A. Andrews, and N. Savoye (2005), Quantification of ^{234}Th recovery in small volume sea water samples by inductively coupled plasma mass spectrometry, *J. Radioanal. Nucl. Chem.*, *263*, 355–360.

Rodriguez y Baena, A. M., S. W. Fowler, and J. C. Miquel (2007), Particulate organic carbon: Natural radionuclide ratios in zooplankton and their freshly produced fecal pellets from the NW Mediterranean (MedFlux 2005), *Limnol. Oceanogr.*, *52*, 966–974.

Rodriguez y Baena, A. M., R. Boudjenoun, S. W. Fowler, J. C. Miquel, P. Masqué, J.-A. Sanchez-Cabeza, and M. Warnau (2008), ^{234}Th-based carbon export during an ice-edge bloom: Sea-ice algae as a likely bias in data interpretation, *Earth Planet. Sci. Lett.*, *269*, 595–603.

Rudels, B., R. D. Muench, J. Gunn, U. Schauer, and H. J. Friedrich (2000), Evolution of the Arctic Ocean boundary current north of the Siberian Shelves, *J. Mar. Syst.*, *25*, 77–99.

Rutgers van der Loeff, M., R. Meyer, B. Rudels, and E. Rachor (2002), Resuspension and particle transport in the benthic nepheloid layer in and near Fram Strait in relation to faunal abundances and ^{234}Th depletion, *Deep-Sea Res., Part I*, *49*, 1941–1958.

Rutgers van der Loeff, M., M. M. Sarin, M. Baskaran, C. Benitez-Nelson, K. O. Buesseler, M. Charette, M. Dai, O. Gustafsson, P. Masque, and P. J. Morris (2006), A review of present techniques and methodological advances in analyzing ^{234}Th in aquatic systems, *Mar. Chem.*, *100*, 190–212.

Savoye, N., C. R. Benitez-Nelson, A. B. Burd, J. K. Cochran, M. A. Charette, K. O. Buesseler, G. A. Jackson, M. Roy-Barman, S. Schmidt, and M. Elskens (2006), ^{234}Th sorption and export models in the water column: A review, *Mar. Chem.*, *100*, 234–249.

Savoye, N., T. W. Trull, S. H. M. Jacquet, J. Navez, and F. Dehairs (2008), ^{234}Th-based export fluxes during a natural iron fertilization experiment in the Southern Ocean (KEOPS). *Deep Sea Res., Part II*, *55*, 841–855.

Thomalla, S., R. Turnewitsch, M. Lucas, and A. Poulton (2006), Particulate organic carbon export from the North and South Atlantic gyres: The ^{234}Th/^{238}U disequilibrium approach, *Deep Sea Res., Part II*, *53*, 1629–1648.

Trimble, S. M., and M. Baskaran (2005), The role of suspended particulate matter in ^{234}Th scavenging and ^{234}Th-derived export fluxes of POC in the Canada Basin of the Arctic Ocean, *Mar. Chem.*, *96*, 1–19.

Wallace, D. W. R., B. Moore, and E. P. Jones (1987), Ventilation of the Arctic Ocean cold halocline: Rates of diapycnal and isopycnal transport, oxygen utilization, and primary production inferred using chlorofluoromethane distribution, *Deep Sea Res., Part A.*, *34*, 1957–1979.

Wassmann, P., et al. (2004), Particulate organic carbon flux to the Arctic sea floor, in *The Organic Carbon Cycle in the Arctic Ocean*, edited by R. Stein and R. W. Macdonald, pp. 101–138, Springer, Berlin.

Zernova, V. V., E.-M. Nöthig, and V. P. Shevshenko (2000), Vertical microalga flux in the northern Laptev Sea, *Oceanology*, *40*, 801–807.

P. Cai, State Key Laboratory of Marine Environmental Science, Xiamen University, Xiamen 361005, China. (caiph@xmu.edu.cn)

K. Lepore, School of Physics, University College Dublin, Belfield, Dublin 5, Ireland.

S. B. Moran, Graduate School of Oceanography, University of Rhode Island, Narragansett, RI 02882, USA.

E.-M. Nöthig, M. Rutgers van der Loeff, and I. Stimac, Alfred-Wegener Institute for Polar and Marine Research, D-27570 Bremerhaven, Germany.